



The Abdus Salam
**International Centre
for Theoretical Physics**



2484-6

ICTP-IAEA Joint Workshop on Nuclear Data for Science and Technology: Medical Applications

30 September - 4 October, 2013

Overview of decay data

NICHOLS Alan Leslie
United Kingdom

α , β^+ , γ and Auger-Electron Decay Data in Nuclear Medicine – Experimental Determination, Status and Deficiencies

A.L. Nichols*

* *affiliated to Department of Physics, Faculty of Engineering and Physical Sciences, University of Surrey, Guildford, GU2 7XH, UK; and Manipal University, Madhav Nagar, Manipal 576104, Karnataka, India.*

Abstract

Cancer treatment represents a major economic and medical issue because of the extensive incidence of the disease worldwide, with a particularly large rate of increase to be found in developing countries – under such unfortunate circumstances, up to half of all cancer patients receive some form of radiation therapy in the course of their treatment. Various facets of the preparation and both evasive and non-evasive delivery and irradiation of patients require sound knowledge and characterisation in order to ensure efficacious treatments. One important requirement is the adoption and implementation of accurate and well-defined nuclear decay data. Nuclear data needs will be described with respect to their importance in ensuring the further evolution of improvements in nuclear medicine throughout the early 21st century. Experimental measurement techniques are reviewed, with the emphasis placed on recent developments that have the potential to achieve substantial leaps in our understanding of the nucleus, particular by means of γ -ray spectroscopy. A select number of internationally-accepted decay-data evaluations and compilations are also discussed in terms of their contents. Various important decay-data issues are assessed, and note taken of any significant requirements for better quantified data. Both the recommendations formulated during the course of recent technical debate and the results of completed and on-going work are described.

Lectures:	Overview of decay data – Part I	11:15, 30 September 2013
	Overview of decay data – Part II	11:00, 1 October 2013
Demonstration:	Data retrieval exercises	16:00, 3 October 2013

12 September 2013

1. Introduction

The suitability of specific radioisotopes for medical applications is well established in relation to cancer diagnosis and therapy [1–3]. Both nuclear reactors and particle accelerators, coupled with powerful chemical separation techniques, provide the means of producing suitable high-purity radioisotopes for diagnostic studies and therapeutic treatment [4, 5]. More specifically, medical applications of radiation are of considerable interest, and therefore over the previous twenty-five years the International Atomic Energy Agency (IAEA) has supported a series of investigations into the identification and quantification of production routes and decay characteristics of those radioisotopes judged to be of existing and emerging importance in nuclear medicine [6, 7]. Recommendations have been formulated during the course of a series of extensive technical discussions, resulting in various completed, on-going and proposed coordinated research projects [8–11].

Prior to consideration of the status and identified deficiencies in the nuclear data adopted to characterise exposure to diagnostic and therapeutic radionuclides in nuclear medicine, consideration is given to the basic needs for accurate and comprehensive decay data judged as important in defining the desired optimum exposure of patients. Well-defined measurements of α , β^- , β^+ , γ , X-ray, and Auger- and conversion-electron emissions are required to avoid both under- and over-exposure to such disparate radiations during the course of diagnostic and radiotherapeutic treatments.

2. Nuclear Decay Data

Accurate measurements and in-depth assessments and evaluations of decay schemes along with the resulting authoritative recommendation of radioactive decay data have been important requirements in nuclear physics over many years. Recommended decay data are normally derived from all relevant publications that include quantification of decay-scheme data primarily by means of direct measurement but also by calculation. The measurement and derivation of such recommended data sets are welcomed by nuclear physicists (a) to define the status and our current knowledge of particular decay parameters, and determine whether there is a need for further study, and (b) hopefully to provide highly reliable input data for modelling codes in order to ensure adoption of their outputs with reasonable confidence.

Atomic and nuclear decay-data parameters encompass the following [12–14]:

- half-life,
- total decay energies (Q-values),
- branching fractions (if more than one known decay mode),
- α -particle energies and emission probabilities,
- β^- -particle energies, emission probabilities and transition types,
- electron-capture and β^+ -particle energies, transition/emission probabilities and transition type (also EC/ β^+ ratios when appropriate),
- γ -ray energies, emission probabilities and internal conversion coefficients (also internal-pair formation coefficients for $\beta^+\beta^-$ when appropriate),
- Auger- and conversion-electron energies and emission probabilities,
- X-ray energies and emission probabilities,
- spontaneous fission properties (branching fraction and recoil energies),
- delayed-neutron energies and emission probabilities,
- delayed-proton energies and emission probabilities, and
- comprehensive quantification of the uncertainties associated with all of the above atomic and nuclear parameters.

Additional ancillary data requirements can be met from the above, including various total mean energies:

- mean heavy-particle energy (includes mean α , neutron, proton, fission fragment, and associated recoil energies),
- mean light-particle energy (includes mean β^- , β^+ , Auger-electron and conversion-electron energies),
- and mean electromagnetic energy (includes mean γ , X-ray, $\beta^+\beta^-$ annihilation radiation and internal bremsstrahlung).

While more exotic modes of decay have been detected (e.g. double-beta ($\beta\beta$) and cluster/heavy-ion decay), these low-probability phenomena are not considered further in this document.

3. Measurements of Decay Data: Experimental Techniques

Radioactive nuclides of interest are normally prepared by means of either reactor irradiation or charged-particle acceleration and controlled bombardment of carefully prepared targetry. Isotopic enrichment of the target material and purification of the resulting product represent important requirements when striving to measure accurate decay data. Various radiochemical procedures have been successfully adopted to achieve elemental separation of the irradiated target, including anion-exchange chromatography, application of many forms of liquid-liquid extraction, and dry distillation [15-17]. For example, the adoption of various radiochemical techniques to achieve high levels of radionuclidic purity was very important in forming the basis for accurate measurements of the positron emission probabilities of ^{64}Cu , ^{76}Br and ^{124}I for medical applications [17].

Long-established experimental techniques can be used to quantify in detail specific features of a decay scheme, ranging from α , γ and electron spectroscopy operated in singles and various coincidence modes, time-dependent measurements of these emissions to determine important parameters such as half-lives, and angular correlation studies for improved understanding of the structure of the nucleus. The more substantive techniques are briefly discussed below with respect to nuclear medicine, along with some thoughts on future developments.

3.1 α spectroscopy

Obviously, measurements of α spectra play an important role in quantifying and defining the decay schemes of α -particle emitting nuclides, and impact most significantly on studies of many heavy elements and actinides. One loss over recent years has been the decline in maintenance of dedicated magnetic spectrometers that offer extremely good energy resolution. Precise, well-defined studies of α spectra were feasible with homogeneous-field magnetic spectrographs [18, 19]. Silicon-based ionization detectors such as the silicon barrier detector (SBD) and passivated implanted planar silicon (PIPS) detector are now much more commonly used to measure the energies and emission probabilities of α particles [20]. As examples, good resolution α spectra obtained by means of a 450-mm² PIPS detector are shown in Fig. 1 for mass-separated sources of ^{237}Np and ^{243}Am [21].

Significant developments have recently occurred with respect to improvements in energy resolution by means of cryogenic microcalorimetry:

- a) detector system consisting of a superconducting transition-edge sensor (TES) with Mo:Cu bilayer and an absorber of superconducting tin has been shown to give an energy resolution of (1.06 ± 0.04) keV FWHM for 5.3-MeV α particles [22];

- b) sensor of gold doped with a small concentration of erbium (Au:Er) for which the magnetization changes as a function of modification in temperature by α -particle absorption – energy resolution of (2.83 ± 0.05) keV FWHM was determined for 5.5-MeV α particles [23].

Such ultra-high resolutions are a significant improvement beyond the theoretical limit of conventional silicon detectors. Alpha-particle measurements with this type of detector system would greatly reduce uncertainties in decay schemes and specific aspects of their decay data, with an inevitably beneficial knock-on effect involving the accuracy and efficacy of their application.

3.2 X- and γ -ray spectroscopy

The extremely successful development and adoption of silicon and germanium crystals as detectors in X- and γ -ray spectroscopy has contributed immensely to our understanding of the atomic nucleus across the known Chart of the Nuclides. Since the late 1960s, Si- and Ge-based detectors have offered the best compromise between energy resolution and efficiency to ensure sound, accurate and reliable X- and γ -ray spectral studies. Example spectra of both γ and electron emissions from a ^{67}Cu source are shown in Fig. 2, as obtained by means of HPGe and thin Si detectors, respectively (Kondev, private communication, ANL, USA, 2013).

More specifically, major advances into the 1980s were associated with increased volume and improved purity of Ge crystals, while the more recent introduction of segmented Ge systems has further improved their detection capabilities and performance characteristics. Thus, a significant amount of nuclear structure data measured and evaluated for inclusion in recommended decay databases originates from γ -ray spectroscopy undertaken with single-crystal Ge(Li) and HPGe detectors which operate satisfactorily below 110K (and therefore are normally maintained by means of liquid nitrogen at 77K). Directly measured data include X- and γ -ray energies and emission probabilities, with the added potential to derive the spins, parities and lifetimes of excited states, determine γ transition types and mixing ratios, and calculate directly other features of the decay scheme under investigation. Low-energy photon spectrometers (LEPS) based on a planar small-area HPGe crystal have also been specifically developed to measure γ -ray spectra over the low to intermediate energy range from 3 to approximately 300 keV at high resolution, and an example γ spectrum of a chemically-purified ^{233}Pa source is shown in Fig. 3 [21].

The division of a Ge crystal into sections offers additional information identified with the γ interactions, referred to as γ -ray tracking expressed in terms of energy, time and location – the net result has been the twin achievements of unprecedented efficiency and energy resolution. The development and operational characteristics of single-crystal Ge detectors and more advanced Ge detector arrays can be found in the substantial review articles of Lee *et al.* [24], and Eberth and Simpson [25]. Only a brief semi-historic summary is given below.

Rapid progress in the discovery and understanding of nuclear structure and decay data in the 1970s was almost entirely related to the advent of Ge(Li) detectors in γ -ray spectroscopy. Such beginnings led on to technological advances in the growth of large high-purity Ge crystals to increase the peak-to-Compton ratio, reduce background effects, and improve the coincidence rate and spectral statistics. Escape-suppression shields were introduced in order to reject partly absorbed events from the γ spectra, and the number of escape-suppressed Ge detectors was increased into arrays during the course of the 1980s to compensate for the commensurate loss in coincidence efficiency [25]. Such HPGe arrays with double gating and ancillary detectors opened up the possibility of measuring γ - γ - γ coincidences to quantify

weak and complex γ cascades. Second-generation systems consisting of 4π solid-angle arrays of germanium detectors and BGO (bismuth germanate ($\text{Bi}_4\text{Ge}_3\text{O}_{12}$)) shields have proved to be very costly, and therefore resulted in the evolution of only two recognised primary projects (Fig. 4):

Gammasphere – multi-laboratory programme based in the USA; and
Euroball collaboration in Europe.

Gammasphere and Euroball are seen as achieving the highest feasible goals for 4π solid-angle arrays with escape-suppressed Ge detectors. Their impressive achievements in the continued evolution and resolution of nuclear structure and decay scheme data can be found on the Web [26, 27].

Scientific interest has tended to focus in recent years on extraordinary N/Z ratios close to the proton and neutron drip lines as a consequence of the growing need to support the study of nuclear reactions generated by emerging radioactive ion beam facilities (RIB). Theoretical analyses and experimental studies on Ge-based detector design has led to the concept of γ -ray tracking in terms of the position, energy and time of all γ -ray interaction points within Ge detector systems (Fig. 5):

- GRETA (Gamma Ray Energy Tracking Array, USA [24]; geodesic configuration of 120 to 130 segmented HPGe detectors);
- AGATA (Advanced Gamma Tracking Array, Europe [25, 28]; geodesic configuration of 180 hexagonal and 12 pentagonal segmented HPGe detectors).

Identification of the interaction points and quantification of the energy deposited at these locations can be achieved with highly-segmented Ge detectors and pulse-shape analyses. However, the sequence of a γ -ray scattering process is too fast for measurement compared with the time resolution of a Ge detector, and therefore tracking algorithms based on the underlying interaction processes have to be used. While GRETA and AGATA will permit access to the farthest reaches of the Chart of the Nuclides, other areas of nuclear application will also benefit from the operational advances in Ge detector technology. Thus, the development of position-sensitive γ -ray detectors for nuclear structure studies will have important repercussions in medical imaging, astrophysics and nuclear safeguards.

GRETINA represents a significant stepping-stone towards GRETA, and consists of coaxial Ge crystals of tapered hexagonal shape that make up seven modules, each containing four 36-fold segmented crystals (Fig. 6). This set of 28 Ge crystals covers a quarter of the 4π solid angle envisaged for GRETA, and will be extensively tested in a series of nuclear structure, reaction and symmetry studies [29]. Similarly, an AGATA sub-array consisting of five triple clusters of highly-segmented Ge detectors has been assembled at Laboratori Nazionali di Legnaro, Padova (total of 15 Ge crystals compares with the full AGATA 4π geometry of 60 triple clusters (180 Ge detectors)). Complementary analysis systems are available to operate in conjunction with the AGATA sub-array, and so extend the measurement capabilities to a broader range of nuclear physics topics [30].

Assembled stacks of planar double-sided Ge strip detectors (DSSD) possess sufficient pixelation to achieve γ -ray positional resolution [24]. Possible drawbacks are envisaged, such as the existence of dead layers at the edge of each planar crystal and the need for mechanical structure to ensure the provision of sufficient cooling to the HPGe detectors. Nevertheless, such systems are being studied for their γ -ray tracking potential and possible application in high-resolution photon imaging.

The ability to discriminate between γ rays of slightly different energies by means of a scintillator is of importance in medical imaging, γ -ray spectroscopy and X-ray astronomy.

Both NaI(Tl) and CsI(Tl) have been the scintillators of choice for over 50 years because of their reasonable energy resolution, while other scintillators such as $\text{Bi}_4\text{Ge}_3\text{O}_{12}$ in positron emission tomography (PET) and PbWO_4 in high-energy nuclear physics have found appropriate application. However, lanthanum halides doped with Ce^{3+} have also been shown to exhibit significant promise based on good energy resolution in combination with fast luminescence decay [31-33]. The superior energy resolution of $\text{LaBr}_3(\text{Ce})$ scintillator has successfully been used with Gammasphere to quantify with good precision the lifetimes of nuclear levels between 50 ps and 1 ns, as populated in the IT and β^- decay of $^{177\text{m}}\text{Lu}$ [34]. Potentially new and improved scintillators are constantly being assessed for adoption in high-resolution γ -ray spectroscopy, and studies of their performance provide essential guidance as to their suitability and application [35].

Another noteworthy technique for accurate X- and low-energy γ -ray detection is the X-ray microcalorimeter [36, 37]. Effectively, the detector system consists of 36 microcalorimeters in 6 x 6 array, although only 32 are electronically active: 28 pixels use 8- μm thick HgTe absorbers, and the remaining four pixels use 30- μm thick Bi absorbers. Maximum sensitivity is achieved when this device operates at 60 mK to give an energy resolution of 6 eV (FWHM) from 0 to 10 keV, while an operating temperature of 90 mK gives FWHM of ~ 26 eV up to about 60 keV. This device senses and quantifies the heat deposited by incident photons on the HgTe absorbers, and has been used with impressive accuracy to determine an energy split of only (7.6 ± 0.5) eV between the ground and first excited states of ^{229}Th , based on precisely measured differences in the more substantial γ rays populating both members of the doublet [38].

3.3 Electron spectroscopy

Appropriate studies of β , Auger-electron and internal conversion-electron emissions have yielded important data in the resolution of difficulties associated with the population and depopulation of daughter nuclear levels and the derivation of a normalisation factor to convert relative γ -ray emission probabilities to absolute values. Various types of detector system have been used, e.g. permanent-magnet 180° spectrograph, permanent-magnet pre-accelerating spectrograph, six-gap spectrometer and iron-free $\pi\sqrt{2}$ double-focusing spectrometer [39-41]. While sound quantification of electron emissions has proved important input to the evolution of fully consistent decay schemes and well-defined decay data, this type of complex spectrometric study has been seriously neglected in recent years. A major problem is the bulky nature of the magnet systems, coupled with the delicate nature of the multi-element detector assemblies – their maintenance and operation have historically proved to be costly.

An alternative approach involves the adoption of electrostatic devices which are more suitable for low-energy electron studies up to 2 keV [42]. Major advantages when compared to magnetic systems include moderate dimensions based on localized electrostatic fields, low-power voltages, robust shielding against external magnetic fields, and insensitivity towards temperature fluctuations. Examples of Auger spectral studies of the KLL, KMM, KMN and KNN transitions of ^{111}Cd from the EC decay of ^{111}In are shown in Figs. 7 and 8 [43-45]. Resolution of the spectral complexity is impressive, with the various components identified in both figures as continuous lines.

β^- intensity distributions are normally determined from any calculated imbalances in the γ population and depopulation of nuclear levels of the decay schemes assembled and quantified by means of γ -ray spectroscopy. However, such experimental studies can be fraught with difficulties resulting from the failure to detect all of the weak γ transitions. Faced with this

basic problem of omission in the study of complex decay schemes, Total Absorption Gamma-ray Spectroscopy (TAGS) has been used to determine unambiguous β^- feeding data [46, 47].

4. Recommended Decay Data

Compilations and evaluations of nuclear data have been produced since the early 1930s to inform and assist nuclear physicists, α and γ spectroscopists, and basic nuclear science researchers. More specifically, extended libraries of reaction cross sections, fission yields, nuclear structure and decay data have evolved in well-defined formats for application by nuclear engineers and plant operators in power generation, fuel reprocessing and waste management. As outlined below, such libraries have historically been updated over agreed time intervals either by means of international consensus, or more localised efforts based on immediate national needs. Regular improvements to and subsequent controlled studies of the contents of a decay-data library also provide a rapid means of assessing their applicability and suitability – such activities assist greatly in defining further requirements to improve existing decay data.

Katharine Way began collecting and compiling nuclear data in the early/mid 1940s, and a compilation of her work first appeared in 1950 [48] – no specific values were recommended, nor uncertainties given. Nevertheless, this work evolved into *Nuclear Data Sheets* (as published by Academic Press, and subsequently by Elsevier Inc.) and the Evaluated Nuclear Structure Data File (ENSDF) [49]. Evaluations of nuclear structure and decay-data measurements are carried out at regular intervals of time, and formatting codes have been developed to display the recommended nuclear data in a clear, concise and well-defined manner. These studies continue as a multinational work programme, with biennial meetings held to discuss both managerial and technical issues under the auspices of the Nuclear Data Section of the International Atomic Energy Agency [50].

4.1 Decay-data files

Consideration has been given to the most comprehensive databases that are judged to be most relevant to defining the status of and existing requirements for improved decay data:

1) ENSDF (Evaluated Nuclear Structure Data File) – consists of nuclear structure and decay data for all known nuclides (www.nndc.bnl.gov/ensdf/). Complete mass chains are evaluated at regular intervals (nominally every seven to ten years) by members of the International Network of Nuclear Structure and Decay Data Evaluators, and published in *Nuclear Data Sheets* [49]. The strength of ENSDF is to be found within the completeness of this comprehensive database (representative contents of ENSDF files are shown in Figs. 9 and 10 for the EC decay data of ^{62}Cu and IT decay data of $^{99}\text{Tc}^{\text{m}}$, respectively). NuDat represents an electronic Chart of the Nuclides based primarily on the contents of ENSDF and constitutes a user-friendly means of accessing decay data (www.nndc.bnl.gov/nudat2/), while MIRD (Medical Internal Radiation Dose) generates the result of processing ENSDF decay data through the RADLST code to give the energies and intensities of all emitted radiation, along with their dose rates (www-nds.iaea.org/mird/). The *Nuclear Wallet Cards* constitute a pocket-sized booklet containing comprehensive sets of selected nuclear properties extracted from ENSDF – Ref. [51] was assembled and issued in 2011. NSR (Nuclear Science References) is an ancillary bibliographic database through which mass-chain evaluators and other users can access all publications of interest (www-nds.iaea.org/nsr/index.jsp).

2) DDEP (Decay Data Evaluation Project) – resulting data files contain comprehensive atomic and nuclear decay data evaluations of selected radionuclides, with emphasis placed on the completeness of each decay scheme and the derivation of X-ray and electron decay data

[52-59]. Multinational evaluations are submitted via a coordinator to the custodian of both the database and associated comments files at the Laboratoire National Henri Becquerel, CEA Saclay, France. DDEP evaluations are based on the implementation of a series of agreed evaluation procedures, with the aim of assembling high-quality files of recommended decay data of immediate value as standards in radionuclide metrology; these particular data sets have also been assessed, adopted and are now supported by the Bureau International des Poids et Mesures (BIPM) as suitably recommended decay data for worldwide adoption. Comprehensive decay data for 201 radionuclides are contained within the DDEP files (www.nucleide.org/DDEP_WG/DDEPdata.htm), as observed on 10 September 2013.

3) Relevant IAEA databases – a number of nuclear data initiatives organised as Coordinated Research Projects (CRPs) under the auspices of the International Atomic Energy Agency (IAEA) have resulted in the generation of high-quality decay data.

- a) Update of X ray and gamma ray decay data standards for detector calibration and other applications, 1998-2005 [60-62]

www-nds.iaea.org/xgamma_standards/

www-nds.iaea.org/publications/tecdocs/sti-pub-1287_Vol1.pdf

www-nds.iaea.org/publications/tecdocs/sti-pub-1287_Vol2.pdf

Radionuclides within this particular database of high relevance to nuclear medicine include ^{60}Co , ^{64}Cu , ^{66}Ga , ^{67}Ga , $^{99\text{m}}\text{Tc}$, ^{111}In , ^{123}I , ^{125}I , ^{131}I , ^{137}Cs , ^{153}Sm , ^{166}Ho , ^{169}Yb , ^{192}Ir and ^{201}Tl [61, 62].

- b) Updated actinide decay data library, 2005-2011 [63-66] – data also forwarded for inclusion in the DDEP database, and listed on the web site

www.nucleide.org/DDEP_WG/DDEPdata.htm

Radionuclides within this particular decay database address requirements in (i) nuclear power generation with the inclusion of all important Th, Pa, U, Np, Pu, Am and Cm radionuclides and their natural decay products, and (ii) nuclear medicine applications identified with ^{212}Bi (^{228}Th decay chain), ^{213}Bi ($^{229}\text{Th}/^{225}\text{Ac}$ decay chain), $^{211}\text{At}/^{211}\text{Po}$, ^{223}Ra (within ^{227}Ac decay chain), ^{241}Am and ^{252}Cf [66].

Other nuclear data libraries have been assembled and subsequently updated in various ways, based primarily on the guidance and requirements of the nuclear power industry. These decay-data sub-libraries have been prepared via a combination of evaluation and direct adoption of recommendations from respected data sources (e.g. data extraction from ENSDF, DDEP and other evaluated atomic and nuclear data files). These recognised nuclear applications databases and their sub-libraries of recommended decay data are maintained in an internationally-accepted format (ENDF-6) and are normally dedicated to the modelling of power-reactor operations and fission-based fuel cycles, although they can be used further afield for fusion research studies and various non-energy applications, if desired.

Communication links with many electronic decay-data files are rapid and comparatively easy to implement in the age of the PC, Internet, CD and DVD. As mentioned above, NuDat provides a user-friendly means of extracting decay data from ENSDF (www.nndc.bnl.gov/nudat2/); LiveChart also accesses ENSDF, and offers the user a wide range of procedures to interrogate this database and display the nuclear parameters of interest in various ways (www-nds.iaea.org/relnsd/vchart/index.html). JANIS constitutes an equivalent software platform for the rapid inspection and display of numerical data within the JEFF nuclear data library (www.oecd-nea.org/janis/).

Dedicated catalogues of γ -ray spectra have been assembled to assist greatly in the characterisation and quantification of the radioactive content of materials [67, 68]. Systematic

studies of the γ -ray emissions of individual radionuclides have been carried out by means of NaI(Tl) scintillation, Si(Li), Ge(Li) and HPGe detectors, and these “fingerprint” spectra are of immense value in spectroscopic analyses. With the advent of the Internet, these γ -ray spectrum catalogues and enhancements have conveniently been made available in electronic form through the Web site: www.inl.gov/gammaray/catalogs/catalogs.shtml

NaI(Tl) scintillator – www.inl.gov/gammaray/catalogs/pdf/naicat.pdf

and Ge and Si(Li) detectors – www.inl.gov/gammaray/catalogs/pdf/gecat.pdf

4.2 Status of decay data

Important work continues or is being planned to explore further structural facets of the nucleus, particularly through the use of radioactive ion beams to study specific areas of the Chart of the Nuclides in a highly focussed manner. Furthermore, significant efforts are constantly being made to respond fully to the demands of decay-data users in support of their nuclear applications. Accurate measurements and sound evaluations of decay data have been proposed and are underway to provide information to assist in basic nuclear physics research and ensure the efficacy and validity of nuclear data as applied to nuclear medicine, analytical science, and fission and fusion reactor physics.

Specific inadequacies and uncertainties remain to be addressed with respect to the decay-scheme data for a number of radionuclides of possible application in nuclear medicine, as discussed below in Section 5. Further work is required to build on previous initiatives such as the relevant IAEA CRPs through consideration of possible needs to improve specific decay-data parameters over the next 5 to 15 years. Greater accuracies in some of the existing data would prove beneficial, along with new additions to ensure that some pre-emptive measures are in place to address our future requirements for diagnosis and radiotherapy.

5. Nuclear Medicine

Both nuclear diagnostic and therapeutic procedures extend across a wide range of medical activities to address and benefit human health in a safe and efficacious manner [1]. Specific radionuclides have been identified as potentially suitable for various life-saving applications. While their production routes and decay properties need to be defined with confidence, some deficiencies remain, especially with regard to the optimum generation of specific radionuclides, minimization or elimination of impurities, and the accurate quantification of various decay parameters [69-71]. Decay-data requirements include a sound knowledge of the half-life and α , β^- , Auger-electron, conversion-electron, β^+ , γ and X-ray energies and emission probabilities as appropriate for patient-dose calculations.

Various radionuclides of the desired purity and decay characteristics have been adopted for the diagnostic imaging of physiological and biochemical processes within the human body. Nuclear techniques such as Single-Photon Emission Computer Tomography (SPECT) and Positron Emission Tomography (PET) complement other imaging methods (e.g. magnetic resonance and ultrasound) to furnish an extremely powerful means of detecting functional abnormalities and disease. A number of γ -emitting radionuclides possess decay characteristics that are highly suitable for diagnostic studies by means of gamma cameras (Table 1) – their chemical form is particularly important in ensuring efficient and precise delivery to the body function(s) of interest.

Table 1: Commonly used radionuclides in nuclear medicine for gamma imaging of body functions: relevant decay properties [49, 52-58].

Radionuclide	Half-life	Noteworthy gamma emissions: E_γ (keV), P_γ (%)
^{67}Ga	3.2617 (5) d	93.307 (12), 38.1 (7)%; 184.577 (17), 20.96 (44)%; 300.232 (21), 16.60 (37)%; 393.528 (20), 4.59 (10)%
$^{81}\text{Rb}/^{81}\text{Kr}^m$ generator	$^{81}\text{Kr}^m$: 13.10 (3) s ^{81}Rb : 4.572 (4) h	190.46 (16), 67.66 (32)%
$^{82}\text{Sr}/^{82}\text{Rb}$ generator	^{82}Rb : 1.2575 (2) min ^{82}Sr : 25.34 (2) d	511 annihilation, 190.9 (4)%; 776.52 (1), 15.08 (16)%
$^{99}\text{Mo}/^{99}\text{Tc}^m$ generator	$^{99}\text{Tc}^m$: 6.0067 (5) h ^{99}Mo : 2.7479 (6) d	140.511 (1), 88.5 (2)%
^{111}In	2.8047 (4) d	171.28 (3), 90.61 (20)%; 245.35 (4), 94.12 (6)%
^{123}I	13.2234 (37) h	158.97 (5), 83.25 (21)%
^{131}I	8.0233 (19) d	80.1850 (19), 2.607 (27)%; 284.305 (5), 6.06 (6)%; 364.489 (5), 81.2 (8)%; 636.989 (4), 7.26 (8)%
^{133}Xe	5.2475 (5) d	80.9979 (11), 37.0 (3)%
^{201}Tl	3.0421 (17) d	135.312 (34), 2.604 (22)%; 167.45 (3), 10.0 (1)%

Cyclotrons and linear accelerators have increasingly been used to generate radionuclides for both diagnostic and therapeutic purposes by means of a wide range of charged-particle reactions [2, 4, 5], along with nuclear reactors employed to produce various activation and fission products for similar applications. Latter examples include sealed sources of ^{60}Co and ^{137}Cs to provide external γ beams that penetrate the body and constitute the means of controlled therapeutic treatment to internal tumours. Studies of heavy-ion beam therapy have furnished striking evidence for the accurate delivery of a well-defined, localised dose to a particular site, and carbon-ion beams exhibit particular promise in this respect. Brachytherapy involves the use of sealed sources placed in or close to the tumour, while attempting to ensure minimal damage to healthy tissue – ^{103}Pd , ^{125}I (as X-ray emitters), and ^{137}Cs and ^{192}Ir (as γ emitters) with effective ranges of a few centimetres are commonly used, while β^- emitters include ^{32}P , ^{90}Y and ^{188}Re with effective ranges of a few millimetres. Radio-immunotherapy involves the covalent bonding and labelling of monoclonal antibodies and peptides with radionuclides such as ^{90}Y , ^{131}I , ^{153}Sm and ^{213}Bi for injection into the bloodstream, followed by transport and attachment to tumours. PET has become an extremely noteworthy and successful technique for the diagnosis of cancer – the most popular radionuclide for such studies has been ^{18}F (half-life of 1.83 h), which requires the radionuclide production and patient treatment facilities to be close to each other geographically.

The proposed introduction of less familiar radionuclides in nuclear medicine necessitates a sound knowledge of their production cross sections, half-lives and decay schemes, and much effort is expended to derive such data through measurement and evaluation. As noted briefly in Section 1, medical applications of radiation are of considerable interest to member states of the International Atomic Energy Agency (IAEA), and therefore from about 1980 onwards the IAEA has supported a series of well-focused discussions and in-depth investigations into the identification and quantification of the production routes and decay characteristics of those radioisotopes judged to be of existing and emerging importance in nuclear medicine. These IAEA initiatives have included a Coordinated Research Project (CRP) on “Charged particle cross-section database for medical radioisotope production: diagnostic radioisotopes and monitor reactions” to consider the nuclear data requirements for diagnostic radionuclides [6], followed by an equivalent study for therapeutic radionuclides defined as “Nuclear data for the

production of therapeutic radionuclides” [7]. While both projects were primarily dedicated to measurements and evaluations of relevant cross sections for product nuclides and impurities, limited amounts of recommended decay data were also tabulated from ENSDF [49].

Re-assessments and further supportive recommendations were formulated during the course of a series of extensive technical debates that began in 2008:

- a) consideration of the existing IAEA database of charged-particle cross sections for diagnostic radioisotopes and monitor reactions (i.e. principal product of the coordinated research project undertaken from 1995 to 2001 [6]), resulting in the establishment of a new coordinated research project in December 2012 to improve and extend the excitation functions of the existing charged-particle monitor reactions and decay data for medical radionuclides [8, 11];
- b) high-precision beta-intensity measurements and evaluations for specific PET radioisotopes for which the decay data of approximately 50 positron-emitting radionuclides were assessed, and recommendations made for a series of measurements and evaluations to improve the known decay characteristics of existing and potential PET radionuclides [9]; and
- c) cross-section and decay-data requirements for medical applications over an intermediate-term timescale of approximately 5 to 15 years, based on extensive discussions in 2011 [10].

Existing recommendations identified with items (a) and (c) focus on cross sections for a reasonably wide range of targets and projectiles, along with highly-specific requirements for further decay data measurements. Item (b) is more clearly related to inadequacies in the measured positron and X-ray emission probabilities of a relatively modest number of existing and potential PET radionuclides.

Continued developments in medical imaging and therapy will involve the utilization of improved diagnostic and therapeutic techniques, along with the production of potentially more effective and suitable radionuclides. Such an envisaged set of circumstances merits the consideration of future needs to expand and improve the content of nuclear databases for medical applications. A summary of the recommendations for improved decay data is given below, based on the envisaged requirements for (a) diagnostic γ -ray emitters, (b) positron emitters, (c) therapeutic β^- , X-ray and γ -ray emitters, (d) therapeutic Auger-electron emitters, and (e) therapeutic α emitters, and covering an estimated timescale of approximately fifteen years up to ~ 2025 . The reader is also referred to the original IAEA reports for the recommended measurements and evaluations of excitation functions in order to optimize the production of these radionuclides [10, 11].

5.1 Charged-particle cross sections for beam-monitoring reactions and diagnostic radionuclides (1995-2001, and 2012 onwards)

A major step change in the medical application of neutron-deficient radionuclides began to occur in the 1960s with the emerging development of judicious combinations of target and accelerated beams of charged particles capable of generating the required products to the desired level of purity. Although these methods of production were well established by the early 1990s, no evaluated and recommended sets of nuclear data were available to assist and guide the medical physicists in their efficacious treatment of life-threatening carcinomas. Under these circumstances, the IAEA organised and supported meetings and studies in the early 1980s that led to the establishment in 1995 of a Coordinated Research Project (CRP) dedicated to the development of a Charged Particle Cross-Section Database for Medical

Radioisotope Production, focusing on diagnostic radionuclides and related beam-monitor reactions and aiming to address the following needs:

- compilation and evaluation of the most important reactions in the monitoring of proton, deuteron, ^3He and alpha particle beams,
- compilation and evaluation of production cross-section data for radionuclides most commonly used in nuclear medicine for diagnosis,
- development of calculational tools for the prediction of unknown cross sections.

The CRP involved eleven experts from nine research institutes and national radionuclide production centres – participants held three research co-ordination meetings from 1995 to 1998 to agree and undertake individual work programmes, and their findings and recommendations were assembled as an appropriate database [6]. Much of the experimental work has been published, along with their consideration in various reviews, e.g. [69, 70]. Cross-section publications for twenty-two monitor reactions were considered, consisting of eight specific and generalized reactions for proton beams, five for deuterons, three for ^3He and six for alpha particles, for which the data were evaluated over the ranges of particle-beam energy specified in Table 2.

Table 2: Charged-particle beam monitor reactions.

Reaction	$t_{1/2}$ of product nucleus	Particle energy range (MeV)
proton		
$^{27}\text{Al}(p,x)^{22}\text{Na}$	2.60 y	30 – 100
$^{27}\text{Al}(p,x)^{24}\text{Na}$	15.0 h	30 – 100
$^{\text{nat}}\text{Ti}(p,x)^{48}\text{V}$	15.97 d	5 – 30
$^{\text{nat}}\text{Ni}(p,x)^{57}\text{Ni}$	1.48 d	15 – 50
$^{\text{nat}}\text{Cu}(p,x)^{56}\text{Co}$	77.24 d	50 – 100
$^{\text{nat}}\text{Cu}(p,x)^{62}\text{Zn}$	9.19 h	14 – 60
$^{\text{nat}}\text{Cu}(p,x)^{63}\text{Zn}$	38.47 min	4.5 – 50
$^{\text{nat}}\text{Cu}(p,x)^{65}\text{Zn}$	243.93 d	2.5 – 100
deuteron		
$^{27}\text{Al}(d,x)^{22}\text{Na}$	2.60 y	29.5 – 80
$^{27}\text{Al}(d,x)^{24}\text{Na}$	15.0 h	15 – 80
$^{\text{nat}}\text{Ti}(d,x)^{48}\text{V}$	15.97 d	9 – 50
$^{\text{nat}}\text{Fe}(d,x)^{56}\text{Co}$	77.24 d	8 – 50
$^{\text{nat}}\text{Ni}(d,x)^{61}\text{Cu}$	3.33 h	2.5 – 50
^3He		
$^{27}\text{Al}(^3\text{He},x)^{22}\text{Na}$	2.60 y	10 – 100
$^{27}\text{Al}(^3\text{He},x)^{24}\text{Na}$	15.0 h	25 – 100
$^{\text{nat}}\text{Ti}(^3\text{He},x)^{48}\text{V}$	15.97 d	16 – 100
α		
$^{27}\text{Al}(\alpha,x)^{22}\text{Na}$	2.60 y	29 – 100
$^{27}\text{Al}(\alpha,x)^{24}\text{Na}$	15.0 h	50 – 100
$^{\text{nat}}\text{Ti}(\alpha,x)^{51}\text{Cr}$	27.70 d	5 – 40
$^{\text{nat}}\text{Cu}(\alpha,x)^{65}\text{Zn}$	243.93 d	15 – 50
$^{\text{nat}}\text{Cu}(\alpha,x)^{66}\text{Ga}$	9.49 h	8 – 30
$^{\text{nat}}\text{Cu}(\alpha,x)^{67}\text{Ga}$	3.26 d	15 – 50

Similar systematic studies of the production cross sections for popular γ and β^+ radionuclides were undertaken as defined in Tables 3 and 4, respectively. All of the experimental data considered are given in Ref. [6], although only those studies judged to be reliable and in acceptably good agreement were used in the subsequent evaluations. The final sets of recommended excitation functions are presented as discrete incremental data in tabulated form, and are also depicted as graphical comparisons with the various original sets of experimental data [6].

Table 3: Production cross sections for γ -emitting diagnostic radionuclides.

Reaction	$t_{1/2}$ of product nucleus	Particle energy range (MeV)
$^{67}\text{Zn}(p,n)^{67}\text{Ga}$	3.26 d	2 – 25
$^{68}\text{Zn}(p,2n)^{67}\text{Ga}$		13 – 30
$^{\text{nat}}\text{Kr}(p,x)^{81}\text{Rb}$	4.57 h	14.5 – 80
$^{82}\text{Kr}(p,2n)^{81}\text{Rb}$		14.5 – 30
$^{111}\text{Cd}(p,n)^{111}\text{In}$	2.80 d	4 – 30
$^{112}\text{Cd}(p,2n)^{111}\text{In}$		11.5 – 35
$^{123}\text{Te}(p,n)^{123}\text{I}$	13.2 h	4 – 20
$^{124}\text{Te}(p,2n)^{123}\text{I}$		12 – 30
$^{124}\text{Te}(p,n)^{124}\text{I}$		6 – 30
$^{127}\text{I}(p,5n)^{123}\text{Xe}(\beta^+/\text{EC})^{123}\text{I}$	2.08 h/13.2 h	37 – 100
$^{124}\text{Xe}(p,pn)^{123}\text{Xe}(\beta^+/\text{EC})^{123}\text{I}$		16.5 – 40
$^{124}\text{Xe}(p,2n)^{123}\text{Cs}(\beta^+/\text{EC})^{123}\text{Xe}(\beta^+/\text{EC})^{123}\text{I}$	5.88 min/2.08 h/13.2 h	15.5 – 40
$^{127}\text{I}(p,3n)^{125}\text{Xe}(\beta^+/\text{EC})^{125}\text{I}$		20 – 100
$^{203}\text{Tl}(p,3n)^{201}\text{Pb}(\beta^+/\text{EC})^{201}\text{Tl}$	9.33 h/3.042 d	18 – 36
$^{203}\text{Tl}(p,2n)^{202}\text{Pb}^{\text{m}}(\beta^+/\text{EC})^{202}\text{Tl}$		9 – 27
$^{203}\text{Tl}(p,4n)^{200}\text{Pb}(\beta^+/\text{EC})^{200}\text{Tl}$	21.5 h/26.1 h	27.5 – 36

Table 4: Production cross sections for β^+ -emitting diagnostic radionuclides.

Reaction	$t_{1/2}$ of product nucleus	Particle energy range (MeV)
$^{14}\text{N}(p,\alpha)^{11}\text{C}$	20.33 min	4 – 25
$^{16}\text{O}(p,\alpha)^{13}\text{N}$	9.965 min	6 – 20
$^{14}\text{N}(d,n)^{15}\text{O}$	2.04 min	1 – 15
$^{15}\text{N}(p,n)^{15}\text{O}$		4 – 20
$^{18}\text{O}(p,n)^{18}\text{F}$	109.8 min	2.5 – 20
$^{\text{nat}}\text{Ne}(d,x)^{18}\text{F}$		1.5 – 21
$^{69}\text{Ga}(p,2n)^{68}\text{Ge}$	270.95 d	13 – 40
$^{\text{nat}}\text{Ga}(p,xn)^{68}\text{Ge}$		11.5 – 60
$^{85}\text{Rb}(p,4n)^{82}\text{Sr}$	25.34 d	36.5 – 70
$^{\text{nat}}\text{Rb}(p,xn)^{82}\text{Sr}$		33 – 100

Nuclear reaction models can be used to predict cross sections when measurements are either not available or exhibit large discrepancies. CRP participants decided to use a number of available models as guides in their studies of almost fifty reactions, rather than adopt the resulting data as a full evaluation (although in some cases the modelled cross sections did indeed become the recommended excitation functions). The calculated cross sections exhibited good agreement with the experimental data for $A > 30$, and also produced better fits for proton-induced reactions compared with deuteron, ^3He and alpha reactions. Poor modelling fits to the lower mass targets may be attributed to the reaction mechanism used in the codes. Nuclear structure plays a critical role in the lighter masses, and the R-matrix theory is more appropriate in the modelling of cross sections for such targets. Therefore, the CRP did not pursue modelling for light targets, and used only experimental data for their evaluations. All of the recommended data that evolved from this CRP can be found on a dedicated and fully-maintained IAEA Web site: www-nds.iaea.org/medportal/

As noted earlier in the text, limited amounts of recommended decay data were also adopted and tabulated from ENSDF [49], and were subsequently manipulated by means of the RADLST program to generate atomic and nuclear radiations associated with the radioactive decay processes [72]. The resulting files contain the energies, intensities and dose rates for the various individual radiations identified with α , β^- , β^+ , electron-capture, γ rays, conversion-electron decay, and electron-positron internal-pair formation. Energies, intensities and dose rates of X rays and Auger electrons are also calculated as contributions to the electron-capture and conversion-electron decay processes. Data are generated in Medical

Internal Radiation Dose (MIRD) format. Examples of the dose rates derived from the evaluated decay data are given in Tables 5, 6 and 7 for ^{18}F , ^{22}Na and ^{123}I , respectively.

Table 5: MIRD dose rate data for ^{18}F as determined from ENSDF decay data [49, 72].

Half-life of 109.77 min		November 1996	
β^+ /EC decay mode		^{18}O daughter is stable	
Radiation	P_i (Bq-s) ⁻¹	Energy (MeV)	$P_i \times E_i$
β_1^+	9.67×10^{-01}	2.498×10^{-01} *	2.42×10^{-01}
γ^\pm	1.93	5.110×10^{-01}	9.89×10^{-01}
K X-ray	1.80×10^{-04}	5.249×10^{-04} *	9.42×10^{-08}
K X-ray	4.74×10^{-12}	5.000×10^{-04} *	2.37×10^{-15}
Auger-K	3.07×10^{-02}	5.200×10^{-04} *	1.60×10^{-05}
Listed X, γ and γ^\pm radiations			9.89×10^{-01}
Listed β , ce and Auger radiations			2.42×10^{-01}
Listed radiations			1.23

* Average energy (MeV).

Table 6: MIRD dose rate data for ^{22}Na as determined from ENSDF decay data [49, 72].

Half-life of 2.6027 y		December 2005	
β^+ /EC decay mode		^{22}Ne daughter is stable	
Radiation	P_i (Bq-s) ⁻¹	Energy (MeV)	$P_i \times E_i$
β_1^+	9.03×10^{-01}	2.155×10^{-01} *	1.95×10^{-01}
β_2^+	5.60×10^{-04}	8.350×10^{-01} *	4.68×10^{-04}
γ^\pm	1.81	5.110×10^{-01}	9.24×10^{-01}
γ_1	9.99×10^{-01}	1.275	1.27
K X-ray	8.98×10^{-04}	8.486×10^{-04} *	7.62×10^{-07}
K X-ray	4.51×10^{-04}	8.486×10^{-04} *	3.83×10^{-07}
Auger-K	8.74×10^{-02}	8.200×10^{-04} *	7.17×10^{-05}
Listed X, γ and γ^\pm radiations			2.20
Listed β , ce and Auger radiations			1.95×10^{-01}
Listed radiations			2.39

* Average energy (MeV).

Table 7: MIRD dose rate data for ^{123}I as determined from ENSDF decay data [49, 72].

Half-life of 13.2234 h		October 2004	
EC decay mode		^{123}Te daughter is radioactive $^{123}\text{Te}^m$ daughter is radioactive – yield of 4.25×10^{-05}	
Radiation	P_i (Bq-s) ⁻¹	Energy (MeV)	$P_i \times E_i$
γ_1	8.33×10^{-01}	1.590×10^{-01}	1.32×10^{-01}
ce-K, γ_1	1.36×10^{-01}	1.272×10^{-01}	1.73×10^{-02}
ce-L, γ_1	1.77×10^{-02}	1.540×10^{-01} a	2.73×10^{-03}
ce-M, γ_1	3.52×10^{-03}	1.580×10^{-01} a	5.57×10^{-04}
ce-N ⁺ , γ_1	8.41×10^{-04}	1.588×10^{-01} a	1.34×10^{-04}
γ_9	7.08×10^{-04}	2.480×10^{-01}	1.76×10^{-04}
γ_{12}	7.91×10^{-04}	2.810×10^{-01}	2.22×10^{-04}
γ_{18}	1.26×10^{-03}	3.464×10^{-01}	4.36×10^{-04}
γ_{21}	4.28×10^{-03}	4.400×10^{-01}	1.88×10^{-03}
γ_{23}	3.16×10^{-03}	5.053×10^{-01}	1.60×10^{-03}
γ_{24}	1.39×10^{-02}	5.290×10^{-01}	7.36×10^{-03}
γ_{25}	3.82×10^{-03}	5.385×10^{-01}	2.05×10^{-03}
γ_{31}	8.33×10^{-04}	6.246×10^{-01}	5.20×10^{-04}
γ_{33}	2.67×10^{-04}	6.880×10^{-01}	1.84×10^{-04}
γ_{34}	6.16×10^{-04}	7.358×10^{-01}	4.54×10^{-04}
γ_{35}	5.91×10^{-04}	7.836×10^{-01}	4.63×10^{-04}
K _{α1} X-ray	4.59×10^{-01}	2.747×10^{-02}	1.26×10^{-02}
K _{α2} X-ray	2.47×10^{-01}	2.720×10^{-02}	6.71×10^{-03}
K β X-ray	1.60×10^{-01}	3.100×10^{-02} *	4.96×10^{-03}

L X-ray	8.98×10^{-02}	3.770×10^{-03} *	3.38×10^{-04}
Auger-K	1.23×10^{-01}	2.270×10^{-02} *	2.80×10^{-03}
Auger-L	9.52×10^{-01}	3.190×10^{-03} *	3.04×10^{-03}
Listed X, γ and γ^\pm radiations			1.72×10^{-01}
Omitted X, γ and γ^\pm radiations **			3.24×10^{-04}
Listed β , ce and Auger radiations			2.66×10^{-02}
Omitted β , ce and Auger radiations **			6.22×10^{-05}
Listed radiations			1.99×10^{-01}
Omitted radiations **			3.86×10^{-04}

* Average energy (MeV).

^a Maximum energy (MeV) for subshell.** Each omitted transition contributes < 0.100% to $\Sigma(P_i \times E_i)$.

Since the completion of the CRP described above, significant developments have occurred in medical imaging techniques and the utilization of additional diagnostic and therapeutic radionuclides. Under these circumstances, further consideration has been given to the increasing study and adoption of somewhat less well-defined β^+ and α emitters. Under these evolving circumstances, a new CRP initiative was launched in December 2012 to instigate a work programme to develop and improve the existing database for charged-particle monitor reactions and medical radioisotope production [11]. Details of this recently established coordinated research project are given in Table 8. As identified in 2011, cross-section requirements are primarily linked to a significant number of emerging γ and β^+ emitters for specialised use in single photon emission computed tomography (SPECT) and positron emission tomography (PET), respectively. These specified needs also include quantification of alternative routes for the production of $^{99}\text{Mo}/^{99}\text{Tc}^m$ as a consequence of concern with respect to an increasing inability to guarantee long-term supply via thermal-neutron fission. Other requests include improved decay data for specialised forms of radiotherapy that include the adoption of α emitters (^{230}U decay chain) and Auger electrons (e.g. ^{103}Pd and ^{111}In). Specific radionuclides would also benefit from comprehensive decay-scheme evaluations to define dose rates accurately and ensure their efficacy (e.g. $^{62,63}\text{Zn}$, ^{76}Br and ^{120}I). Well-defined cross sections and decay data remain an important facet of the work, and agreement was reached to derive uncertainties and covariances for the resulting recommended data sets. Recommended decay-data studies are listed as bold type in Table 8.

Table 8: Agreed production cross sections and decay data studies for IAEA coordinated research project, December 2012 [11]; decay-data studies highlighted in bold type.

Cross sections	Decay data	Comments
monitor reactions		
$^{27}\text{Al}(p,x)^{22,24}\text{Na}$	–	include isotope activity ratios up to beam energy of 800 MeV
$^{27}\text{Al}(d,x)^{22,24}\text{Na}$		include isotope activity ratios
$^{27}\text{Al}(^3\text{He},x)^{22,24}\text{Na}$		higher energies up to 100 MeV
$^{27}\text{Al}(\alpha,x)^{22,24}\text{Na}$		
$^{\text{nat}}\text{Ti}(d,x)^{46}\text{Sc}$	–	high energy deuterons
$^{\text{nat}}\text{Ti}(^3\text{He},x)^{48}\text{V}$	–	measurements and re-assessment up to 46 MeV
$^{\text{nat}}\text{Ni}(d,x)^{56,58}\text{Co}$	–	
$^{\text{nat}}\text{Cu}(p,x)^{58}\text{Co}$		energies > 50 MeV
$^{\text{nat}}\text{Cu}(p,x)^{62,63,65}\text{Zn}$	$^{62,63}\text{Zn}$	inconsistencies – resolve with respect to isotope activity ratios; evaluation of $^{62,63}\text{Zn}$ decay schemes
$^{\text{nat}}\text{Cu}(d,x)^{62,63,65}\text{Zn}$		
$^{\text{nat}}\text{Cu}(\alpha,x)^{66,67}\text{Ga}$, ^{65}Zn		
$^{\text{nat}}\text{Mo}(p,x)^{96\text{r},g+m}\text{Tc}$	–	
–	^{61}Cu	evaluation of ^{61}Cu decay scheme
diagnostic γ emitters		
$^{90}\text{Zr}(n,p)^{90}\text{Y}^{g+m}$	–	consider new measurements for data validation and production
$^{100}\text{Mo}(n,2n)^{99}\text{Mo}$	–	consider new measurements for data validation and production
$^{100}\text{Mo}(p,2n)^{99}\text{Tc}^{g+m}$		evaluation
$^{100}\text{Mo}(p,pn)^{99}\text{Mo}$		evaluation
$^{100}\text{Mo}(d,3n)^{99}\text{Tc}^{g+m}$		evaluation
$^{100}\text{Mo}(d,p2n)^{99}\text{Mo}$		evaluation
$^{100}\text{Mo}(\gamma,n)^{99}\text{Mo}$		

$^{238}\text{U}(\gamma, f)^{99}\text{Mo}$ –	$^{99}\text{Tc}^m$	evaluation of Auger-electron decay data
$^{51}\text{V}(p, n)^{51}\text{Cr}$ $^{na}\text{Fe}(p, x)^{51}\text{Cr}$	–	
$^{64}\text{Zn}(n, p)^{64}\text{Cu}$	–	
$^{67}\text{Zn}(n, p)^{67}\text{Cu}$ $^{68}\text{Zn}(n, x)^{67}\text{Cu}$ $^{68}\text{Zn}(\gamma, p)^{67}\text{Cu}$	^{67}Cu	evaluation of ^{67}Cu decay scheme
$^{112}\text{Cd}(p, 2n)^{111}\text{In}$	^{111}In	new measurements and evaluation; evaluation of Auger-electron decay data
$^{124}\text{Xe}(p, 2n)^{123}\text{Cs}$ $^{124}\text{Xe}(p, pn)^{123}\text{Xe}$ $^{124}\text{Xe}(p, x)^{121}\text{I}$	–	^{123}I production - re-evaluation ^{123}I production - re-evaluation ^{123}I production – evaluation of side reaction (contaminant)
$^{na}\text{W}(\alpha, x)^{186, 188}\text{Re}$	–	
$^{203}\text{Tl}(p, 2n)^{202}\text{Pb}^m$ $^{203}\text{Tl}(p, 3n)^{201}\text{Pb}$ $^{203}\text{Tl}(p, 4n)^{200}\text{Pb}$	–	
β^+ emitters $^{55}\text{Mn}(p, 4n)^{52}\text{Fe}$ $^{na}\text{Ni}(p, x)^{52}\text{Fe}$ $^{52}\text{Cr}(\alpha, \text{He}, 3n)^{52}\text{Fe}$	^{52}Fe	assess if new measurements required, and evaluation of ^{52}Fe decay scheme
$^{58}\text{Ni}(p, \alpha)^{55}\text{Co}$ $^{54}\text{Fe}(d, n)^{55}\text{Co}$ $^{56}\text{Fe}(p, 2n)^{55}\text{Co}$ $^{na}\text{Fe}(p, x)^{55}\text{Co}$	–	
$^{61}\text{Ni}(p, n)^{61}\text{Cu}$ $^{64}\text{Zn}(p, \alpha)^{61}\text{Cu}$ –	–	
$^{66}\text{Zn}(p, n)^{66}\text{Ga}$ $^{63}\text{Cu}(\alpha, n)^{66}\text{Ga}$	^{66}Ga	discrepancy in measurements of intensity of weak gamma line measurement of positron intensities, and evaluation of ^{66}Ga decay scheme
$^{68}\text{Zn}(p, n)^{68}\text{Ga}$ $^{65}\text{Cu}(\alpha, n)^{68}\text{Ga}$	–	
$^{na}\text{Ge}(p, xn)^{72}\text{As}$	^{72}As	measurement of positron intensities, and evaluation of ^{72}As decay scheme
$^{75}\text{As}(p, 3n)^{73}\text{Se}$ $^{72}\text{Ge}(\alpha, 3n)^{73}\text{Se}$	^{73}Se	measurement of main positron intensity, and evaluation of ^{73}Se decay scheme
$^{76}\text{Se}(p, n)^{76}\text{Br}$ $^{77}\text{Se}(p, 2n)^{76}\text{Br}$ $^{75}\text{As}(\alpha, 3n)^{76}\text{Br}$	^{76}Br	measurement of positron intensities, and evaluation of ^{76}Br decay scheme
$^{86}\text{Sr}(p, n)^{86}\text{Y}$ $^{88}\text{Sr}(p, 3n)^{86}\text{Y}$ $^{85}\text{Rb}(\alpha, 3n)^{86}\text{Y}$	^{86}Y	PET analogue of therapeutic ^{90}Y measurement of positron intensities, and evaluation of ^{86}Y decay scheme
$^{89}\text{Y}(p, n)^{89}\text{Zr}$ $^{89}\text{Y}(d, 2n)^{89}\text{Zr}$ $^{na}\text{Y}(\alpha, x)^{89}\text{Zr}$ $^{89}\text{Y}(\alpha, x)^{90}\text{Nb}$ $^{93}\text{Nb}(p, x)^{90}\text{Nb}$	^{89}Zr	evaluation of ^{89}Zr decay scheme
$^{94}\text{Mo}(p, n)^{94}\text{Tc}^m$ $^{92}\text{Mo}(\alpha, x)^{94}\text{Tc}^m$	$^{94}\text{Tc}^m$	PET analogue of therapeutic $^{99}\text{Tc}^m$ evaluation of $^{94}\text{Tc}^m$ decay scheme
$^{110}\text{Cd}(p, n)^{110}\text{In}^m$	–	
$^{120}\text{Te}(p, n)^{120}\text{I}$ $^{122}\text{Te}(p, 3n)^{120}\text{I}$	^{120}I	evaluation of ^{120}I decay scheme
β^+ generators $^{44}\text{Ti}/^{44}\text{Sc}$ generator	^{44}Ti	evaluation of ^{44}Ti half-life
$^{52}\text{Fe}/^{52}\text{Mn}^m$ generator: $^{55}\text{Mn}(p, 4n)^{52}\text{Fe}$ $^{na}\text{Ni}(p, x)^{52}\text{Fe}$ $^{52}\text{Cr}(\alpha, \text{He}, 3n)^{52}\text{Fe}$	–	
$^{62}\text{Zn}/^{62}\text{Cu}$ generator: $^{63}\text{Cu}(p, 2n)^{62}\text{Zn}$	–	PET analogue of therapeutic ^{67}Cu
$^{68}\text{Ge}/^{68}\text{Ga}$ generator: $^{na}\text{Ga}(p, xn)^{68}\text{Ge}$ $^{69}\text{Ga}(p, 2n)^{68}\text{Ge}$ $^{71}\text{Ga}(p, 4n)^{68}\text{Ge}$	–	PET analogue of therapeutic ^{67}Ga new measurements, and evaluation new measurements, and evaluation new measurements, and evaluation
$^{72}\text{Se}/^{72}\text{As}$ generator: $^{75}\text{As}(p, 4n)^{72}\text{Se}$ $^{na}\text{Br}(p, x)^{72}\text{Se}$	–	
$^{82}\text{Sr}/^{82}\text{Rb}$ generator: $^{85}\text{Rb}(p, 4n)^{82}\text{Sr}$ $^{na}\text{Rb}(p, xn)^{82}\text{Sr}$	–	
$^{110}\text{Sn}/^{110}\text{In}^m$ generator	–	PET analogue of therapeutic ^{111}In and $^{114}\text{In}^m$
$^{118}\text{Te}/^{118}\text{Sb}$ generator	–	PET analogue of proposed/new therapeutic ^{117}Sb and ^{119}Sb
$^{122}\text{Xe}/^{122}\text{I}$ generator	–	PET analogue of therapeutic ^{123}I, ^{125}I and ^{131}I
$^{128}\text{Ba}/^{128}\text{Cs}$ generator	–	PET analogue of proposed/new therapeutic ^{131}Cs
$^{140}\text{Nd}/^{140}\text{Pr}$ generator	–	

α emitters $^{229}\text{Th}(\alpha)^{225}\text{Ra}(\beta^-)^{225}\text{Ac}(\alpha)$ decay chain to ^{213}Bi : $^{232}\text{Th}(p,x)^{225}\text{Ra}$ $^{232}\text{Th}(p,x)^{225}\text{Ac}$ $^{226}\text{Ra}(p,2n)^{225}\text{Ac}$ $^{232}\text{Th}(p,x)^{227}\text{Ac}$	–	new measurements up to 200 MeV, and evaluation new measurements up to 200 MeV, and evaluation additional measurements, and evaluation long-lived ^{227}Ac impurity (21.8 y), and contaminant in ^{225}Ac
$^{230}\text{U}(\alpha)^{226}\text{Th}(\alpha)$ decay chain $^{231}\text{Pa}(\text{d},3n)^{230}\text{U}$ $^{231}\text{Pa}(p,2n)^{230}\text{U}$ $^{232}\text{Th}(p,3n)^{230}\text{Pa}(\beta^-)^{230}\text{U}$	^{230}U decay chain	new measurements, and evaluation; evaluation of all decay schemes within ^{230}U decay chain new measurements, and evaluation ^{230}Pa β^- branch of 7.8% – new measurements, and evaluation
$^{227}\text{Th}(\alpha)^{223}\text{Ra}(\alpha)$ decay chain $^{232}\text{Th}(p,x)^{227}\text{Th}$	–	new measurements, and evaluation
electron and X-ray emitters $^{130}\text{Ba}(n,\gamma)^{131}\text{Ba}(\text{EC})^{131}\text{Cs}$ $^{131}\text{Xe}(p,n)^{131}\text{Cs}$ $^{133}\text{Cs}(p,3n)^{131}\text{Ba}(\text{EC})^{131}\text{Cs}$	–	
$^{176}\text{Hf}(\alpha,2n)^{178}\text{W}(\text{EC})^{178}\text{Ta}$ $^{\text{nat}}\text{Hf}(p,x)^{178}\text{Ta}$	^{178}Ta	evaluation of Auger-electron decay data
–	^{103}Pd	evaluation of ^{103}Pd decay scheme, including Auger-electron data

5.2 Charged-particle cross sections for therapeutic radionuclides (2003-2011)

Following the successful completion in 2001 of the cross-section studies outlined above, consideration was given to equivalent nuclear data needs in therapeutic treatments. Agreement was reached in 2003 to extend this type of work to neutron and charged-particle induced reactions to produce appropriate radionuclides after consideration of both current and potentially future requirements. Thus, a second coordinated research project was launched, with virtually identical technical aims to the earlier CRP, involving the active participation of nineteen experts from eleven research institutes. Three research co-ordination meetings were held between 2003 and 2006 to agree and undertake individual work programmes, and the findings and recommendations were assembled in the form of an IAEA technical report and accessible database [7].

All relevant data were assembled and evaluated for almost 30 thermal-neutron capture reactions to produce 18 radionuclides and one contaminant formed in a thermal reactor core. Similar extensive exercises were also conducted for over 30 charged-particle induced reactions to generate 15 radionuclides and three possible contaminants. These established and emerging radionuclides and the evaluated nuclear reactions are listed in Tables 9 and 10, respectively.

Table 9: Production cross sections and fission yields for established therapeutic radionuclides [7].

Reaction	$t_{1/2}$ of product nucleus	Production route
$^{31}\text{P}(n,\gamma)^{32}\text{P}$	14.26 d	thermal reactor
$^{32}\text{S}(n,p)^{32}\text{P}$		thermal reactor and accelerator
$^{89}\text{Y}(n,p)^{89}\text{Sr}$	50.53 d	thermal reactor and accelerator
$^{89}\text{Y}(n,\gamma)^{90}\text{Y}$	64.05 h	thermal reactor
$^{90}\text{Zr}(n,p)^{90}\text{Y}$		thermal reactor and accelerator
$^{235}\text{U}(n,f)^{90}\text{Sr}(\beta^-)^{90}\text{Y}$	28.90 y/64.05 h	thermal reactor
$^{102}\text{Pd}(n,\gamma)^{103}\text{Pd}$	17.0 d	thermal reactor
$^{103}\text{Rh}(p,n)^{103}\text{Pd}$		accelerator
$^{103}\text{Rh}(d,2n)^{103}\text{Pd}$		accelerator
$^{103}\text{Rh}(p,x)^{102}\text{Rh}^{g+m}$	207.3 d and 3.74 y	accelerator
$^{103}\text{Rh}(d,x)^{102}\text{Rh}^{g+m}$	contaminants in ^{103}Pd	accelerator
$^{124}\text{Xe}(n,\gamma)^{125}\text{Xe}(\beta^+/\text{EC})^{125}\text{I}$	16.9 h/59.41 d	thermal reactor
$^{125}\text{I}(n,\gamma)^{126}\text{I}$	12.9 d contaminant in ^{125}I	thermal reactor
$^{130}\text{Te}(n,\gamma)^{131}\text{Te}(\beta^-)^{131}\text{I}$	25.0 min/8.0 d	thermal reactor
$^{235}\text{U}(n,f)^{131}\text{I}$	8.0 d	thermal reactor
$^{235}\text{U}(n,f)^{137}\text{Cs}$	30.1 y	thermal reactor

$^{152}\text{Sm}(n,\gamma)^{153}\text{Sm}$	46.28 h	thermal reactor
$^{153}\text{Eu}(n,p)^{153}\text{Sm}$		thermal reactor
$^{185}\text{Re}(n,\gamma)^{186}\text{Re}$	3.72 d	thermal reactor
$^{186}\text{W}(p,n)^{186}\text{Re}$		accelerator
$^{186}\text{W}(d,2n)^{186}\text{Re}$		accelerator
$^{187}\text{Re}(n,\gamma)^{188}\text{Re}$	17.00 h	thermal reactor
$^{186}\text{W}(n,\gamma)^{187}\text{W}(n,\gamma)^{188}\text{W}(\beta^-)^{188}\text{Re}$	69.8 d/17.00 h	thermal reactor
$^{191}\text{Ir}(n,\gamma)^{192}\text{Ir}$	73.8 d	thermal reactor
$^{192}\text{Os}(p,n)^{192}\text{Ir}^{g+m1}$		accelerator
$^{192}\text{Os}(d,2n)^{192}\text{Ir}^{g+m1}$		accelerator

Table 10: Production cross sections for emerging therapeutic radionuclides [7].

Reaction	$t_{1/2}$ of product nucleus	Production route
$^{63}\text{Cu}(n,\gamma)^{64}\text{Cu}$	12.70 h	thermal reactor
$^{64}\text{Ni}(p,n)^{64}\text{Cu}$		accelerator
$^{64}\text{Ni}(d,2n)^{64}\text{Cu}$		accelerator
$^{64}\text{Zn}(n,p)^{64}\text{Cu}$		thermal reactor
$^{nat}\text{Zn}(d,x)^{64}\text{Cu}$		accelerator
$^{68}\text{Zn}(p,2p3n)^{64}\text{Cu}$		accelerator
$^{68}\text{Zn}(p,x)^{64}\text{Cu}$		accelerator
$^{67}\text{Zn}(n,p)^{67}\text{Cu}$	61.8 h	thermal reactor
$^{68}\text{Zn}(p,2p)^{67}\text{Cu}$		accelerator
$^{70}\text{Zn}(p,\alpha)^{67}\text{Cu}$		accelerator
$^{67}\text{Zn}(p,n)^{67}\text{Ga}$	3.26 d	accelerator
$^{68}\text{Zn}(p,2n)^{67}\text{Ga}$		accelerator
$^{86}\text{Sr}(p,n)^{86}\text{Y}$	14.74 h	accelerator
$^{104}\text{Ru}(n,\gamma)^{105}\text{Ru}(\beta^-)^{105}\text{Rh}$	4.44 h/35.36 h	thermal reactor
$^{111}\text{Cd}(p,n)^{111}\text{In}$	2.80 d	accelerator
$^{112}\text{Cd}(p,2n)^{111}\text{In}$		accelerator
$^{113}\text{In}(n,\gamma)^{114}\text{In}^m$	49.5 d	thermal reactor
$^{114}\text{Cd}(p,n)^{114}\text{In}^m$		accelerator
$^{114}\text{Cd}(d,2n)^{114}\text{In}^m$		accelerator
$^{116}\text{Cd}(p,3n)^{114}\text{In}^m$		accelerator
$^{124}\text{Te}(p,n)^{124}\text{I}$	4.18 d	accelerator
$^{124}\text{Te}(d,2n)^{124}\text{I}$		accelerator
$^{125}\text{Te}(p,2n)^{124}\text{I}$		accelerator
$^{125}\text{Te}(p,n)^{125}\text{I}$	59.41 d contaminant in ^{124}I	accelerator
$^{124}\text{Te}(d,n)^{125}\text{I}$	59.41 d contaminant in ^{124}I	accelerator
$^{125}\text{Te}(p,xn)^{124,125}\text{I}$	4.18 d/59.41 d	accelerator
$^{148}\text{Nd}(n,\gamma)^{149}\text{Nd}(\beta^-)^{149}\text{Pm}$	53.1 h	thermal reactor
$^{164}\text{Dy}(n,\gamma)^{165}\text{Dy}(n,\gamma)^{166}\text{Dy}(\beta^-)^{166}\text{Ho}$	81.6 h/26.8 h	thermal reactor
$^{168}\text{Yb}(n,\gamma)^{169}\text{Yb}$	32.0 d	thermal reactor
$^{169}\text{Tm}(p,n)^{169}\text{Yb}$		accelerator
$^{169}\text{Tm}(d,2n)^{169}\text{Yb}$		accelerator
$^{176}\text{Lu}(n,\gamma)^{177}\text{Lu}$	6.65 d	thermal reactor
$^{176}\text{Yb}(d,n)^{177}\text{Lu}$		accelerator
$^{176}\text{Yb}(d,x)^{177}\text{Lu}$		accelerator
$^{176}\text{Yb}(n,\gamma)^{177}\text{Yb}(\beta^-)^{177}\text{Lu}$	1.91 h/6.65 d	thermal reactor
$^{176}\text{Yb}(d,p)^{177}\text{Yb}(\beta^-)^{177}\text{Lu}$		accelerator
$^{233}\text{U}/^{225}\text{Ac}$ decay chain \rightarrow ^{213}Bi	45.6 min	thermal reactor and natural decay
$^{209}\text{Bi}(\alpha,2n)^{211}\text{At}$	7.21 h	accelerator
$^{209}\text{Bi}(\alpha,3n)^{210}\text{At}$	8.1 h contaminant in ^{211}At	accelerator
$^{226}\text{Ra}(p,2n)^{225}\text{Ac}$	10.0 d	accelerator
$^{233}\text{U} \rightarrow ^{229}\text{Th} \rightarrow ^{225}\text{Ra} \rightarrow ^{225}\text{Ac}$	14.9 d/10.0 d	thermal reactor and natural decay

Inadequate cross-section data were found for some of the nuclear processes, and specific radionuclides required investigative measurements, sometimes via alternative reaction routes. Thus, significant amounts of new experimental data were generated during the course of the CRP. Recommended excitation functions are tabulated in discrete digital form, and are also

compared in graphical presentations with the original sets of experimental data included in the evaluation process [7]. Other specific reactions that generate adjacent impurities were also handled in a similar manner. The recommended cross sections and yields are accurate enough to meet the demands of most of the envisaged applications, and can be found on the dedicated IAEA Web site: www-nds.iaea.org/medportal/

As noted earlier in the text, limited amounts of recommended decay data were also adopted and tabulated from ENSDF [49], and were subsequently manipulated by means of the RADLST program to generate dose rates for the atomic and nuclear radiations associated with the radioactive decay processes [72]. The resulting files contain the energies, intensities and dose rates for the various individual radiations identified with α , β^- , β^+ , electron-capture, γ rays, conversion-electron decay, and electron-positron internal-pair formation. Energies, intensities and dose rates of X rays and Auger electrons are also calculated as contributions to the electron-capture and conversion-electron decay processes. Data are generated in Medical Internal Radiation Dose (MIRD) format. Examples of the dose rates derived from the evaluated decay data are given in Tables 11 and 12 for ^{103}Pd and ^{213}Bi , respectively.

Table 11: MIRD dose rate data for ^{103}Pd as determined from ENSDF decay data [49, 72].

Half-life of 16.991 d		October 2009	
EC decay mode		^{103}Rh daughter is stable	
Radiation	P_i (Bq-s) ⁻¹	Energy (MeV)	$P_i \times E_i$
γ_1	6.83×10^{-04}	3.975×10^{-02}	2.71×10^{-05}
ce-K, γ_1	9.52×10^{-02}	1.653×10^{-02}	1.57×10^{-03}
ce-L, γ_1	7.12×10^{-01}	3.634×10^{-02} a	2.59×10^{-02}
ce-M, γ_1	1.44×10^{-01}	3.912×10^{-02} a	5.62×10^{-03}
γ_2	2.73×10^{-07}	5.329×10^{-02}	1.46×10^{-08}
γ_3	1.04×10^{-05}	6.241×10^{-02}	6.48×10^{-07}
ce-K, γ_3	1.19×10^{-05}	3.919×10^{-02}	4.68×10^{-07}
ce-L, γ_3	1.56×10^{-06}	5.900×10^{-02} a	9.19×10^{-08}
ce-M, γ_3	2.73×10^{-07}	6.178×10^{-02} a	1.69×10^{-08}
ce-N ⁺ , γ_3	5.33×10^{-08}	6.233×10^{-02} a	2.71×10^{-05}
γ_4	4.78×10^{-09}	2.419×10^{-01}	1.16×10^{-09}
γ_5	2.80×10^{-05}	2.950×10^{-01}	8.26×10^{-06}
γ_6	1.50×10^{-07}	3.177×10^{-01}	4.77×10^{-08}
γ_7	2.21×10^{-04}	3.575×10^{-01}	7.89×10^{-05}
ce-K, γ_7	2.21×10^{-06}	3.342×10^{-01}	7.37×10^{-07}
ce-L, γ_7	3.97×10^{-07}	3.540×10^{-01} a	1.41×10^{-07}
ce-M, γ_7	7.50×10^{-08}	3.568×10^{-01} a	2.68×10^{-08}
γ_8	1.50×10^{-07}	4.438×10^{-01}	6.67×10^{-08}
γ_9	3.96×10^{-05}	4.971×10^{-01}	1.97×10^{-05}
$K_{\alpha 1}$ X-ray	4.19×10^{-01}	2.022×10^{-02}	8.46×10^{-03}
$K_{\alpha 2}$ X-ray	2.21×10^{-01}	2.007×10^{-02}	4.44×10^{-03}
K_{β} X-ray	1.33×10^{-01}	2.270×10^{-02} *	3.01×10^{-03}
L X-ray	8.73×10^{-02}	2.700×10^{-03} *	2.36×10^{-04}
Auger-K	1.82×10^{-01}	1.700×10^{-02} *	3.09×10^{-03}
Auger-L	1.68	2.390×10^{-03} *	4.02×10^{-03}
Listed X, γ and γ^{\pm} radiations			1.63×10^{-02}
Listed β , ce and Auger radiations			4.02×10^{-02}
Listed radiations			5.65×10^{-02}

* Average energy (MeV).

^a Maximum energy (MeV) for subshell.

Table 12: MIRSD dose rate data for ^{213}Bi as determined from ENSDF decay data [49, 72].

Half-life of 45.59 min α and β^- decay modes		^{209}Tl daughter is radioactive ^{213}Po daughter is radioactive	α November 1991 β^- April 2007
Radiation	P_i (Bq-s) ⁻¹	Energy (MeV)	$P_i \times E_i$
α_1	1.55×10^{-03}	5.549	8.58×10^{-03}
α recoil	1.55×10^{-03}	1.053×10^{-01}	1.63×10^{-04}
α_2	1.94×10^{-02}	5.869	1.14×10^{-01}
α recoil	1.94×10^{-02}	1.114×10^{-01}	2.16×10^{-03}
γ_1	1.27×10^{-04}	8.680×10^{-01}	1.11×10^{-04}
β^-_3	5.86×10^{-03}	9.080×10^{-02} *	5.32×10^{-04}
β^-_8	3.07×10^{-01}	3.204×10^{-01} *	9.85×10^{-02}
β^-_9	2.29×10^{-03}	3.768×10^{-01} *	8.62×10^{-04}
β^-_{10}	6.58×10^{-01}	4.922×10^{-01} *	3.24×10^{-01}
γ_1	4.29×10^{-03}	2.928×10^{-01}	1.26×10^{-03}
γ_2	1.65×10^{-03}	3.238×10^{-01}	5.33×10^{-04}
γ_4	1.65×10^{-04}	5.449×10^{-01}	9.00×10^{-05}
γ_5	2.50×10^{-05}	5.749×10^{-01}	1.44×10^{-05}
γ_6	4.20×10^{-05}	6.009×10^{-01}	2.52×10^{-05}
γ_7	2.30×10^{-05}	6.049×10^{-01}	1.39×10^{-05}
γ_8	3.61×10^{-04}	6.598×10^{-01}	2.38×10^{-04}
γ_9	1.11×10^{-04}	7.108×10^{-01}	7.89×10^{-05}
γ_{10}	2.92×10^{-03}	8.074×10^{-01}	2.36×10^{-03}
γ_{11}	7.10×10^{-05}	8.265×10^{-01}	5.87×10^{-05}
γ_{12}	1.11×10^{-04}	8.680×10^{-01}	9.63×10^{-05}
γ_{14}	5.30×10^{-04}	1.004	5.32×10^{-04}
γ_{15}	1.80×10^{-04}	1.046	1.88×10^{-04}
γ_{16}	2.59×10^{-03}	1.100	2.85×10^{-03}
γ_{17}	5.20×10^{-04}	1.119	5.82×10^{-04}
$K_{\alpha 1}$ X-ray	1.83×10^{-02}	7.929×10^{-02}	1.45×10^{-03}
$K_{\alpha 2}$ X-ray	1.10×10^{-02}	7.686×10^{-02}	8.45×10^{-04}
K_{β} X-ray	8.27×10^{-03}	8.980×10^{-02} *	7.43×10^{-04}
L X-ray	1.55×10^{-02}	1.110×10^{-02} *	1.72×10^{-04}
Listed X, γ and γ^\pm radiations			1.22×10^{-02}
Omitted X, γ , and γ^\pm radiations**			1.48×10^{-05}
Listed β , ce and Auger radiations			4.24×10^{-01}
Omitted β , ce, and Auger radiations**			7.74×10^{-04}
Listed α radiations			1.22×10^{-01}
Listed radiations			5.58×10^{-01}
Omitted radiations**			7.89×10^{-04}

* Average energy (MeV).

** Each omitted transition contributes < 0.100% to $\Sigma(P_i \times E_i)$.**5.3 High-precision beta-intensity measurements and evaluations for positron emission tomography: IAEA report INDC(NDS)-0535, December 2008 [9]**

Along with the commonly used short-lived positron emitters (^{11}C , ^{13}N , ^{15}O and ^{18}F), many useful and potentially useful longer-lived positron emitters have been identified as suitable for application in positron emission tomography (PET), especially diagnoses within neurology, cardiology and oncology. As identified and assessed, the decay data of all of these radionuclides are reasonably well-defined, but there are some remaining deficiencies, especially with regard to quantification of their positron emission probabilities. Both positron energies and emission probabilities have a direct impact on the resolution and quantification of any PET study. Under these circumstances, known decay data for longer-lived positron emitters were critically reviewed by consultants brought together at an IAEA meeting held in Vienna from 3 to 5 September 2008 [9] – thus, requirements for new measurements and evaluations were identified and recommended, as outlined below.

5.3.1 Standard positron emitters

^{11}C , ^{13}N , ^{15}O and ^{18}F are the four commonly used positron-emitting radionuclides produced by means of cyclotrons, possessing well-defined decay characteristics that do not appear to merit further study for PET applications. While both ^{68}Ga and ^{82}Rb obtained from $^{68}\text{Ge}/^{68}\text{Ga}$ and $^{82}\text{Sr}/^{82}\text{Rb}$ generators, respectively, have increased in importance as positron emitters, these systems possess well-characterised decay schemes that do not merit immediate concern.

5.3.2 Non-standard positron emitters

A wide range of potentially suitable radionuclides have been either adopted or proposed that fall within the definition of non-standard positron emitters. These emerging radionuclides were identified during the course of the specialists' discussions, and the following pronouncements were made with respect to the status of their nuclear data and envisaged requirements to improve matters, if necessary:

- ^{57}Ni – recommend measurements of half-life, X-ray and β^+ emission probabilities, and subsequent evaluation of decay scheme;
- ^{66}Ga , ^{72}As , ^{73}Se , ^{86}Y and $^{94}\text{Tc}^{\text{m}}$ – recommend measurements of their X-ray and β^+ emission probabilities, and subsequent evaluations of their decay schemes;
- ^{81}Rb , $^{82}\text{Rb}^{\text{m}}$ and ^{83}Sr possess inaccurately defined decay data (Tables 13 and 14 list β^+ decay data for $^{82}\text{Rb}^{\text{m}}$ and ^{83}Sr , respectively [49]) – require further measurements and subsequent evaluations of their decay schemes;
- ^{75}Br and ^{77}Kr – both of these relatively short-lived radionuclides require additional experimental studies of their β^+ emission probabilities;
- ^{64}Cu – require measurements of the emission probability of the 1345.8-keV γ ray, followed by a full decay-scheme evaluation;
- ^{76}Br and ^{120}I – recommend evaluations of their decay schemes;
- ^{22}Na , ^{30}P , $^{34}\text{Cl}^{\text{m}}$, ^{38}K , ^{45}Ti , ^{48}V , ^{49}Cr , ^{51}Mn , ^{52}Mn , $^{52}\text{Mn}^{\text{m}}$, ^{52}Fe , ^{55}Co , ^{61}Cu , ^{90}Nb , $^{110}\text{In}^{\text{m}}$, ^{124}I and ^{152}Tb are judged to possess reasonably well-defined decay data and adequately evaluated decay schemes (representative β^+ decay data are shown in Table 15 for ^{152}Tb [49]);
- $^{44}\text{Ti}/^{44}\text{Sc}$, $^{62}\text{Zn}/^{62}\text{Cu}$, $^{140}\text{Nd}/^{140}\text{Pr}$ generator systems have well-defined and adequately evaluated decay schemes.

Table 13: Positron decay data of $^{82}\text{Rb}^{\text{m}}$ [49].

Radionuclide	Half-life	End-point energy (keV)	Positron emission probability (%)
$^{82}\text{Rb}^{\text{m}}$	6.472 (6) h	409 (7)	0.0020 (20)
		436 (7)	0.17 (4)
		527 (7)	0.029 (6)
		597 (7)	0.042 (7)
		619 (7)	0.61 (8)
		649 (7)	0.027 (5)
		798 (7)	19.7 (16)
		891 (7)	0.021 (21)
		899 (7)	0.18 (3)
		1020 (7)	0.03 (3)
		1353 (7)	0.18 (18)
1626 (7)	0.20 (20)		
			Σ 21.2 (16)

Table 14: Positron decay data of ^{83}Sr [49].

Radionuclide	Half-life	End-point energy (keV)	Positron emission probability (%)
^{83}Sr	32.41 (3) h	200 (6)	0.00024 (12)
		210 (6)	0.00005 (5)
		217 (6)	0.0004 (4)
		449 (6)	0.9 (4)
		494 (6)	0.012 (6)
		517 (6)	0.0021 (11)
		689 (6)	0.023 (12)
		830 (6)	3.1 (16)
		865 (6)	0.014 (9)
		1155 (6)	0.010 (10)
		1212 (6)	9 (6)
		1254 (6)	13 (19)*

* Although quantified to be $\approx 0\%$ in Ref. [49], can be defined as 13% with a large uncertainty from total β^+ intensity.

Table 15: Positron decay data of ^{152}Tb [49].

Radionuclide	Half-life	End-point energy (keV)	Positron emission probability (%)
^{152}Tb	17.5 (1) h	528 (15)	0.0039 (6)
		563 (15)	0.0020 (3)
		581 (15)	0.019 (3)
		626 (15)	0.0018 (3)
		816 (15)	0.0160 (20)
		852 (15)	0.0058 (11)
		887 (15)	0.110 (10)
		913 (15)	0.0092 (17)
		966 (15)	0.068 (6)
		988 (15)	0.0110 (20)
		1020 (15)	0.0049 (9)
		1056 (15)	0.0150 (20)
		1136 (15)	0.046 (5)
		1185 (15)	0.140 (20)
		1222 (15)	0.190 (16)
		1278 (15)	0.0074 (10)
		1394 (15)	0.082 (11)
		1510 (15)	0.40 (5)
		1513 (15)	0.16 (3)
		1546 (15)	0.013 (3)
		1705 (15)	0.43 (9)
		1719 (15)	0.61 (8)
		1780 (15)	0.08 (3)
1897 (15)	1.90 (20)		
2073 (15)	0.12 (4)		
2213 (15)	0.87 (12)		
2484 (15)	5.5 (6)		
2828 (15)	6.2 (18)		
			Σ 17 (2)

5.3.3 Very short-lived positron emitters formed in hadron therapy

^{10}C , ^{14}O , ^{17}F and $^{18,19}\text{Ne}$ are very short-lived positron emitters formed in hadron therapy, along with ^{11}C , ^{13}N , ^{15}O and ^{18}F . Decay data for these additional radionuclides are entirely adequate for medical purposes.

^{64}Cu , ^{86}Y and ^{124}I are currently considered to be the three most important non-standard radionuclides for PET applications. More specifically, ^{86}Y has gained importance with respect to the clinical dosimetry of ^{90}Y internal radiotherapy; ^{64}Cu is successfully evolving from the point of view of beneficial compound chelation, with a short half-life, single positron energy and insignificant γ -ray emissions; and ^{124}I possesses suitable chemical properties for incorporation within organic molecules that are known to possess highly specific and selective transport properties within the human body. Under such circumstances, every effort should be made to ensure that their nuclear data in particular are accurately defined.

^{72}As , ^{73}Se , ^{76}Br and ^{120}I are of increasing importance for PET studies, while $^{94}\text{Tc}^{\text{m}}$ has proved to be of value in the clinical quantification of $^{99}\text{Tc}^{\text{m}}$ radiopharmaceuticals. Finally, $^{34}\text{Cl}^{\text{m}}$, ^{57}Ni , ^{62}Cu , ^{66}Ga , ^{81}Rb , $^{82}\text{Rb}^{\text{m}}$ and ^{83}Sr were concluded to be of potential significance in future PET diagnoses. Positron emission probability data for all of these radionuclides need to be known with confidence to be of optimum benefit to patients.

5.4 Intermediate-term cross-section and decay data requirements: IAEA report INDC(NDS)-0596, September 2011 [10]

Additional nuclear data consultations under the auspices of the IAEA concerning medical applications focused in 2011 on intermediate- and longer-term requirements for excitation functions and decay data [10]. As in earlier such exercises, a wide range of radionuclides were considered on the basis of their decay characteristics and possible application in nuclear medicine:

- (a) diagnostic γ -ray emitters,
- (b) β^+ emitters,
- (c) therapeutic β^- , X-ray and γ -ray emitters,
- (d) therapeutic Auger-electron emitters, and
- (e) therapeutic α emitters.

Definitive summaries of the nuclear data needs for each of the above categories of radionuclide are given in Tables 16 to 20.

5.4.1 Diagnostic γ -ray emitters

Reactor-produced $^{99}\text{Tc}^{\text{m}}$ is the most commonly used γ -ray emitting radionuclide for diagnostic purposes, and both the fission-yield production and decay data are well known. However, new data requirements have arisen as a consequence of recent efforts to produce this radionuclide by means of charged-particle accelerators. Neutron-, proton-, deuteron-, photofission- and photoneutron-induced reactions need to be experimentally studied, and cross-section studies are required, especially with respect to possible radioactive contaminants. Auger-electron and other low-energy electron decay data are also required to assess and possibly develop therapeutic microdosimetry.

Cross-section measurements and evaluations are required for the production of ^{97}Ru and ^{147}Gd by means of ^3He and ^4He beams. Furthermore, the accurate quantification of Auger-electron emissions may become an issue for ^{123}I , if such therapeutic applications arise in the future.

5.4.2 β^+ emitters

Nuclear data needs for established and emerging β^+ emitters are wide ranging. Extensive cross-section and decay-data measurements and evaluations are required for ^{57}Ni , ^{66}Ga , ^{72}As , ^{73}Se , ^{75}Br , ^{76}Br , ^{77}Kr , ^{81}Rb , $^{82}\text{Rb}^{\text{m}}$, ^{83}Sr , ^{89}Zr , $^{94}\text{Tc}^{\text{m}}$ and ^{121}I , and $^{44}\text{Ti}/^{44}\text{Sc}$, $^{52}\text{Fe}/^{52}\text{Mn}^{\text{m}}$, $^{62}\text{Zn}/^{62}\text{Cu}$, $^{72}\text{Se}/^{72}\text{As}$ and $^{140}\text{Nd}/^{140}\text{Pr}$ generators. Cross-section evaluations and decay-data measurements and evaluations are required for ^{86}Y and ^{120}I .

Both cross-section measurements and evaluations are required for the production of ^{95}Ru by means of ^3He and ^4He beams, while cross-section measurements and evaluations for ^{11}C , ^{13}N , ^{14}O , ^{15}O , ^{30}P and ^{38}K need to be extended to proton-beam energies up to 250 MeV (see also Section 5.4.6, below). Furthermore, cross-section measurements and evaluations are required for the production of $^{34}\text{Cl}^m$, ^{43}Sc , ^{45}Ti , ^{48}V , ^{49}Cr , ^{51}Mn , ^{52}Mn , ^{68}Ga , ^{90}Nb and ^{152}Tb , and $^{68}\text{Ge}/^{68}\text{Ga}$ and $^{82}\text{Sr}/^{82}\text{Rb}$ generators, whereas only cross-section evaluations are merited for ^{52}Fe , ^{55}Co , ^{61}Cu and $^{110}\text{In}^m$.

5.4.3 Therapeutic β^- , X-ray and γ -ray emitters

Focus was placed on β^- emitters with known discrepant nuclear data. Thus, both cross-section and decay-data measurements and evaluations are recommended for ^{169}Er and ^{175}Yb , while only cross-section measurements and evaluations are merited for ^{47}Sc , ^{131}Cs , ^{131}Ba and ^{166}Ho , and decay-data measurements and evaluations for ^{67}Cu , ^{103}Pd and ^{161}Tb . The $^{191}\text{Os}/^{191}\text{Ir}^m$ and $^{191}\text{Pt}/^{191}\text{Ir}^m$ generators would benefit from cross-section measurements and evaluations, along with decay-data measurements and evaluation of ^{191}Pt parent for the latter system.

5.4.4 Therapeutic Auger-electron emitters

^{125}I is the most commonly used Auger-electron emitter for internal radiotherapy, and both reactor-production and decay data are well characterized. While all of the following radionuclides were identified as potentially suitable for application with respect to microdosimetry at the molecular and cellular levels, they require much improved Auger-electron decay data: ^{71}Ge , ^{178}Ta , $^{193}\text{Pt}^m$, $^{195}\text{Pt}^m$ and ^{197}Hg (all along with cross-section measurements), and ^{67}Ga , ^{77}Br , $^{99}\text{Tc}^m$, ^{103}Pd , ^{111}In , ^{123}I and ^{140}Nd .

5.4.5 Therapeutic α emitters

Both cross-section measurements and evaluations of the spallation and heavy-ion reactions to produce ^{149}Tb are required, as are cross-section measurements at higher energies and evaluation of the spallation reaction on ^{232}Th to achieve the optimum generation of $^{225}\text{Ac}/^{213}\text{Bi}$. Cross-section measurements and evaluations for $^{232}\text{Th}(p,x)$ production of $^{227}\text{Ac}/^{223}\text{Ra}$ would also prove beneficial. Improved production and characterization of the $^{230}\text{U}/^{226}\text{Th}$ decay chain requires additional cross-section and decay-data measurements and evaluations.

5.4.6 Proton therapy

Consideration was also given to the nuclear data needs identified with proton-beam therapy up to 250 MeV, which were defined as follows:

- (1) non-elastic cross sections of the light elements (C, N and O) at proton energies up to 250 MeV; and
- (2) activation cross sections of residual nuclei, particularly the positron-emitters ^{11}C , ^{13}N , ^{15}O , ^{30}P and ^{38}K .

Relevant experimental data are scarce, especially for proton-beam energies above 20 MeV. Therefore, the best course of action would appear to be the development of more precise models and validated parameter sets tested against available experimental data at the lower proton energies. Such a derivation of better models and validated parameters would be a sound approach, in order to undertake more precise Monte-Carlo transport calculations of the effects on dose deposition of variations in morphology and structure that arise from bone and implants.

Table 16: Diagnostic radionuclides: γ emitters.

Radionuclide	Production data	Decay data [†]	CRP [*]	Comments
^{99m} Tc	¹⁰⁰ Mo(p,2n): evaluation required. ¹⁰⁰ Mo(p, α n) and (p, α): new measurements required before re-evaluation. Impurities: ⁹⁸ Mo(p,2n) ^{97m} Tc: measurements required. ¹⁰⁰ Mo(p,3n) ⁹⁸ Tc and (p,4n) ⁹⁷ Tc: difficult measurements required – theoretical calculations may suffice.	Decay data evaluated in previous IAEA CRP (X-ray and Gamma-ray Decay Data Standards). Data required for Auger electrons ($E_c < 25$ keV) and other low-energy electrons ($E_c < 1$ keV) for microdosimetry (see Table 19).	√	Data requirements to focus on accelerator production – such studies required, especially with regard to impurities. Availability of highly enriched ¹⁰⁰ Mo (>99%) should be investigated.
	¹⁰⁰ Mo(d,3n) ^{99m} Tc and (d,p2n) ⁹⁹ Mo – evaluations required.		√	Limited applicability arises from sparse availability of suitable accelerators.
	¹⁰⁰ Mo(n,2n) ⁹⁹ Mo data: new measurements required for neutron generation by deuterons on carbon targets.		√	(n,2n) reaction product of low specific activity.
	Photofission- and photoneutron-induced reactions to produce ⁹⁹ Mo.		√	(γ ,n) reaction product of low specific activity; (γ ,f) reaction more suitable, but has low cross section.
⁹⁷ Ru	³ He and ⁴ He beams on Mo: measurements and evaluations required.			Limited application.
¹²³ I	Evaluated in previous IAEA CRP (Charged-particle Cross-section Database for Medical Radioisotope Production: Diagnostic Radioisotopes and Monitor Reactions, IAEA-TECDOC-1211, 2001).	Decay data evaluated in previous IAEA CRP (X-ray and Gamma-ray Decay Data Standards). Auger-electron emissions may become an issue to be addressed in the future (see Table 19).	√	Several production reactions will be studied in planned IAEA CRP (nuclear data for charged-particle monitor reactions and medical isotope production; see also INDC(NDS)-0591, 2011) – observed discrepancies will also be investigated further.
¹⁴⁷ Gd	⁴ He beam on Sm, and proton beam on Eu: measurements and evaluations required.	Extremely complex gamma-ray decay scheme.		Special application in MRI + SPECT.
²⁰³ Pb	Production data are known.			Special application in tracer studies.

[†] All decay scheme data should be rigorously assessed to ensure their suitability with respect to decay characteristics, data uncertainties and completeness.

^{*} Symbol √ denotes relevant studies undertaken as part of either a completed or on-going IAEA CRP.

Table 17: β^+ emitters.

Radionuclide	Production data	Decay data [†]	CRP [*]	Comments
¹¹ C, ¹³ N, ^{14,15} O, ³⁰ P, ³⁸ K	Measurements and evaluations required of activation cross sections for proton-induced reactions with energies up to 250 MeV.			Cross sections are well defined for proton-induced reactions with $E_p < 20$ MeV; however, higher energies up to 250 MeV are of interest for proton therapy.
³⁴ Cl ^m	Measurements and evaluations required.			Low priority radionuclide.
⁴³ Sc	Measurements and evaluations required.	Good positron-decay characteristics.		Although difficult to produce, ⁴³ Sc would potentially be very useful.
⁴⁵ Ti, ⁴⁸ V, ⁴⁹ Cr, ⁹⁰ Nb	Measurements and evaluations required.			Potentially important for radioimmunotherapy.
^{51,52} Mn	Measurements and evaluations required.			Special application in MRI + PET.
⁵² Fe, ⁵⁵ Co, ⁶¹ Cu, ¹¹⁰ In ^m	Evaluations required.		√	Several novel applications.
⁵⁷ Ni, ⁷² As, ⁷³ Se, ⁹⁴ Tc ^m	Measurements and evaluations required.	Measurements and evaluation of positron and X-ray emission probabilities required.	√	Priority 2 decay-data evaluation in planned IAEA CRP (nuclear data for charged-particle monitor reactions and medical isotope production; see also INDC(NDS)-0591, 2011).
⁶⁴ Cu	Evaluated in previous IAEA CRP (Nuclear Data for the Production of Therapeutic Radionuclides, IAEA Technical Reports Series No. 473, 2011).		√	Important positron emitter, especially for radioimmunotherapy.
⁶⁶ Ga	Measurements and evaluations required.	Measurements and evaluation of positron and X-ray emission probabilities required.	√	Priority 1 decay-data evaluation in planned IAEA CRP (nuclear data for charged-particle monitor reactions and medical isotope production; see also INDC(NDS)-0591, 2011).
⁶⁸ Ga	Measurements and evaluations required.		√	Direct production of ⁶⁸ Ga is attracting attention, as well as the ⁶⁸ Ge/ ⁶⁸ Ga generator route, because of increased application.
⁷⁵ Br, ⁷⁷ Kr	Measurements and evaluations required.	Measurements and evaluation of positron and X-ray emission probabilities required.		Limited application.
⁷⁶ Br, ⁸⁹ Zr	Measurements and evaluations required.	Measurements and evaluation of positron and X-ray emission probabilities required.	√	Priority 3 decay-data evaluation in planned IAEA CRP (nuclear data for charged-particle monitor reactions and medical isotope production; see also INDC(NDS)-0591, 2011).
⁸¹ Rb, ⁸² Rb ^m , ⁸³ Sr	Measurements and evaluations required.	Measurements and evaluation of positron and X-ray emission probabilities required.		Limited application.
⁸⁶ Y	Evaluations required.	Measurements and evaluation of positron and X-ray emission probabilities required.	√	Important positron emitter for quantification of dosimetry calculations. Priority 1 decay-data evaluation in planned CRP (nuclear data for charged-particle monitor reactions and medical isotope production; see also INDC(NDS)-0591, 2011).
⁹⁵ Ru	³ He and ⁴ He beams: measurements and evaluations.	Many gamma emissions, together with ~14% positron emission probability.		Limited application.
¹²⁰ I ^g	Evaluations required.	Measurements and evaluation of positron and X-ray emission probabilities required.	√	Priority 3 decay-data evaluation in planned CRP (nuclear data for charged-particle monitor reactions and medical isotope production; see also INDC(NDS)-0591, 2011).

Table 17: β^+ emitters (continued).

Radionuclide	Production data	Decay data [†]	CRP [*]	Comments
¹²¹ I	Measurements and evaluations required.	Many gamma emissions, together with ~11% positron emission.		Easier to produce than ¹²⁰ I. Borderline - for longer-term consideration.
¹²⁴ I	Evaluated in previous IAEA CRP (Nuclear Data for the Production of Therapeutic Radionuclides, IAEA Technical Reports Series No. 473, 2011).			Important positron emitter for quantification of dosimetry calculations.
¹⁵² Tb	Measurements and evaluations required.			Potentially useful as lanthanide-based positron emitter.
β^+ generators:				
⁴⁴ Ti/ ⁴⁴ Sc	Measurements and evaluations required.	Evaluation required of parent T _{1/2} .		Long-lived parent (T _{1/2} of 60 y); difficult to produce.
⁵² Fe/ ⁵² Mn ^m	Measurements and evaluations required.	Measurements and evaluation required.		Special application in MRI + PET.
⁶² Zn/ ⁶² Cu	Measurements and evaluations required.	Measurements and evaluation of positron and X-ray emission probabilities of daughter required.	√	Priority 2 decay-data evaluation in planned CRP (nuclear data for charged-particle monitor reactions and medical isotope production; see also INDC(NDS)-0591, 2011).
⁶⁸ Ge/ ⁶⁸ Ga, ⁸² Str/ ⁸² Rb	Measurements and evaluations required.		√	Well-established systems, but databases inadequate.
⁷² Se/ ⁷² As	Measurements and evaluation required.	Measurements and evaluation of positron and X-ray emission probabilities required.	√	Priority 2 decay-data evaluation in planned IAEA CRP (nuclear data for charged-particle monitor reactions and medical isotope production; see also INDC(NDS)-0591, 2011).
¹⁴⁰ Nd/ ¹⁴⁰ Pr	Measurements and evaluation required.	Auger-electron and other low-energy electron data required for ¹⁴⁰ Nd microdosimetry.		Radiotherapy + PET. Parent ¹⁴⁰ Nd(EC) to operate as therapeutic radionuclide, while ¹⁴⁰ Pr is a positron emitter (<i>in-vivo</i> generator).

[†] All decay scheme data should be rigorously assessed to ensure their suitability with respect to decay characteristics, data uncertainties and completeness.

^{*} Symbol √ denotes relevant studies undertaken as part of either a completed or on-going IAEA CRP.

Table 18: Therapeutic β^- and X-ray/ γ emitters.

Radionuclide	Production data	Decay data [†]	CRP [*]	Comments
⁴⁷ Sc	Measurements and evaluations required.			Low-energy β^- emitter.
⁶⁷ Cu	Evaluated in previous IAEA CRP (Nuclear Data for the Production of Therapeutic Radionuclides, IAEA Technical Reports Series No. 473, 2011).	Measurements and evaluation required, particularly with respect to the ground state to ground state transition.		Important radionuclide – emission of low-energy β^- particles, and preparation of organometallic complexes.
¹⁰³ Pd	Evaluated in previous IAEA CRP (Nuclear Data for the Production of Therapeutic Radionuclides, IAEA Technical Reports Series No. 473, 2011).	Data discrepancies – measurements and evaluation required.	√	Priority 1 decay-data evaluation in planned IAEA CRP (nuclear data for charged-particle monitor reactions and medical isotope production; see also INDC(NDS)-0591, 2011). Also included as Auger-electron emitter in Table 19.
¹³¹ Cs	Measurements and evaluations required.		√	X-ray emitter.
¹³¹ Ba	Measurements and evaluations required.	Complex decay scheme requires assessment.	√	X-ray emitter.
¹⁶¹ Tb	¹⁶⁰ Gd(n, γ) ¹⁶¹ Gd(β^-) ¹⁶¹ Tb	Measurements and evaluation required.		Low-energy β^- emitter.
¹⁶⁶ Ho	Evaluated in previous IAEA CRP for reactor production only (Nuclear Data for the Production of Therapeutic Radionuclides, IAEA Technical Reports Series No. 473, 2011). ¹⁶⁴ Dy(2n, γ) ¹⁶⁶ Dy(β^-) ¹⁶⁶ Ho: measurements and evaluation required.	¹⁶⁶ Ho decay data evaluated in previous IAEA CRP (X-ray and Gamma-ray Decay Data Standards).		High-flux reactor required for double-neutron capture.
¹⁶⁹ Er	Measurements and evaluations required, including spallation beam cross sections.	Measurements and evaluation required.		Low-energy β^- emitter.
¹⁷⁵ Yb	Measurements and evaluations required for charged-particle reactions.	Measurements and evaluation required.		Low-energy β^- emitter.
¹⁹¹ Os/ ¹⁹¹ Ir ^m	Measurements and evaluations required.			Low-energy β^- emitter for radiotherapy + SPECT. Potential <i>in-vivo</i> generator. Difficult to produce by means of charged-particle reactions.
¹⁹¹ Pt/ ¹⁹¹ Ir ^m	Measurements and evaluations required.	Measurements and evaluation required of parent decay data.		X-ray emitter. Potential <i>in-vivo</i> generator. Difficult to produce by means of charged-particle reactions.

[†] All decay scheme data should be rigorously assessed to ensure their suitability with respect to decay characteristics, data uncertainties and completeness.

^{*} Symbol √ denotes relevant studies undertaken as part of either a completed or on-going IAEA CRP.

Table 19: Therapeutic Auger-electron emitters.

Radionuclide	Production data	Decay data [†]	CRP [*]	Comments
⁶⁷ Ga, ¹¹¹ In	Evaluated in two previous IAEA CRPs (Charged-particle Cross-section Database for Medical Radioisotope Production: Diagnostic Radioisotopes and Monitor Reactions, IAEA-TECDOC-1211, 2001 (⁶⁷ Ga and ¹¹¹ In), and Nuclear Data for the Production of Therapeutic Radionuclides, IAEA Technical Reports Series No. 473, 2011 (⁶⁷ Ga)).	Auger-electron emissions may become an issue to be addressed in the future.		Previously used in diagnostic studies, both ⁶⁷ Ga and ¹¹¹ In are finding increased application in internal radiotherapy.
⁷¹ Ge	Measurements and evaluations required.	Auger-electron emissions may become an issue to be addressed in the future.		Half-life is rather long at 11.4 d.
⁷⁷ Br	Several reactions have been investigated – evaluations required.	Auger-electron emissions may become an issue to be addressed in the future.		
^{99m} Tc	Commonly available – data needs will only arise if produced by charged-particle reactions on accelerators.	Decay data evaluated in previous IAEA CRP (X-ray and Gamma-ray Decay Data Standards). Data required for Auger electrons ($E_e < 25$ keV) and other low-energy electrons ($E_e < 1$ keV) for microdosimetry.		While regularly used for diagnosis, there is increased application in therapeutics.
¹⁰³ Pd	Evaluated in previous IAEA CRP (Nuclear Data for the Production of Therapeutic Radionuclides, IAEA Technical Reports Series No. 473, 2011).	Measurements and evaluations required.	√	Priority 1 decay-data evaluation in planned IAEA CRP (nuclear data for charged-particle monitor reactions and medical isotope production; see also INDC(NDS)-0591, 2011).
¹²³ I	Evaluated in previous IAEA CRP (Charged-particle Cross-section Database for Medical Radioisotope Production: Diagnostic Radioisotopes and Monitor Reactions, IAEA-TECDOC-1211, 2001).	Auger-electron emissions may become an issue to be addressed in the future.		While regularly used for diagnosis, there is increased application in therapeutics.
¹⁴⁰ Nd	Several reactions have been investigated – evaluations required.	Auger-electron emissions may become an issue to be addressed in the future.		Auger-electron and EC decay. <i>In-vivo</i> generator (¹⁴⁰ Pr) – see Table 17.
¹⁷⁸ Ta	¹⁷⁶ Hf($\alpha, 2n$) ¹⁷⁸ W(EC) ¹⁷⁸ Ta	Auger-electron emissions may become an issue to be addressed in the future.		Auger-electron and EC decay. <i>In-vivo</i> generator (¹⁷⁸ W).
^{193m} Pt, ^{195m} Pt	Measurements and evaluations required.	Auger-electron emissions may become an issue to be addressed in the future.		Large number of Auger electrons emitted.
¹⁹⁷ Hg	Measurements and evaluations required.	Auger-electron emissions may become an issue to be addressed in the future. Measurements and evaluation required.		

[†] All decay scheme data should be rigorously assessed to ensure their suitability with respect to decay characteristics, data uncertainties and completeness.

^{*} Symbol √ denotes relevant studies undertaken as part of either a completed or on-going IAEA CRP.

Table 20: Therapeutic α emitters.

Radionuclide	Production data	Decay data [†]	CRP [*]	Comments
¹⁴⁹ Tb	Measurements and evaluations of spallation and heavy-ion beam reactions.			Emission of low-energy alpha particles (< 4 MeV) renders ¹⁴⁹ Tb potentially useful for special applications.
²¹¹ At/ ²¹¹ Po	Evaluated in previous IAEA CRP (Nuclear Data for the Production of Therapeutic Radionuclides, IAEA Technical Reports Series No. 473, 2011).	²¹¹ At and ²¹¹ Po decay data evaluated in IAEA CRP (Library of Recommended Actinide Decay Data, 2011).		Well-established therapeutic radionuclide.
²²⁵ Ac/ ²¹³ Bi	Lack of cross-section data at higher energies for spallation reaction on ²³² Th.	Full decay chain evaluated in IAEA CRP (Library of Recommended Actinide Decay Data, 2011).	√	Potentially important therapeutic radionuclide.
²²⁷ Ac/ ²²³ Ra	Inadequate cross-section database for ²³² Th(p,x) production of ²²⁷ Ac.	Experimental data and evaluation required for ²²⁷ Ac. ²²³ Ra evaluated in IAEA CRP (Library of Recommended Actinide Decay Data, 2011).	√	Impurity in ²²⁵ Ac production.
²³⁰ U/ ²²⁶ Th	Production reactions will be studied within planned IAEA CRP (nuclear data for charged-particle monitor reactions and medical isotope production).	²³⁰ U decay chain requires evaluation.	√	Decay-data evaluations for ²³⁰ U decay chain were not included in IAEA CRP dedicated to “Library of Recommended Actinide Decay Data, 2011”.

[†] All decay scheme data should be rigorously assessed to ensure their suitability with respect to decay characteristics, data uncertainties and completeness.

^{*} Symbol √ denotes relevant studies undertaken as part of either a completed or on-going IAEA CRP.

6. Concluding Remarks

Extremely significant developments in the field of nuclear medicine are taking place that involve both organ imaging and internal radionuclide therapy. The dynamic and quantitative nature of positron tomography (PET) is being coupled with X-ray tomography (CT) and magnetic resonance imaging (MRI) to provide a highly powerful combination of detector systems for organ imaging. New possibilities for improved internal radiotherapy are also being assessed and developed in terms of two proposed procedures:

- (a) a combination of PET and therapy involving radioimmuno reactions, and
- (b) Auger-electron and α -particle therapy at the cellular level.

Future success with these methods of treatment is difficult to gauge, which impacts significantly on the ability to identify intermediate- and long-term nuclear data needs defined somewhat loosely as within the next 5 to 15 years. Such data needs in nuclear medicine will depend upon the relative success of proposed technological developments and the commensurate identification of suitable radionuclides for medical treatments. Overall, demands are expected to move towards positron emitters and therapeutic radionuclides as outlined in Section 5.4, resulting in the increased adoption of metallic-based positron emitters as a consequence of developments in organometallic-complex chemistry (especially for appropriate Ti, Ga and Cu radionuclides). Furthermore, the adoption of highly-focused therapeutic treatment by means of microdosimetry techniques will also require improved characterisation and quantification of the atomic and nuclear decay data of the most suitable low-energy Auger-electron emitters.

Radionuclides production in the foreseeable future will require intermediate-energy, high-power accelerators with extended proton energies up to 200 MeV. Small cyclotrons operating to a maximum of 30 MeV will not suffice for a significant number of the radionuclides now being considered. Furthermore, there will be a need for such facilities to generate deuteron, ^3He and ^4He particle beams in order to extend the range of production and improve radionuclidic purity. Activation products relevant to proton and heavy-ion radiotherapy will also need to be better quantified with respect to their production cross sections (particularly such positron-emitters as ^{11}C , ^{13}N , ^{15}O , ^{30}P and ^{38}K). A comprehensive calculational route needs to be developed to determine the energies and emission probabilities of the low-energy X-rays and Auger electrons to a higher degree of detail and consistency than is available at present. The aim should be to produce a definitive and consistent set of data of all the nuclides of immediate value to the medical profession. All of the resulting recommended decay schemes should also be used in cross-section and activity measurements.

Recommendations over the previous 15 years have focused on the need for cross-section studies over a reasonably wide range of targets and projectiles, along with decay data measurements for specific radionuclides. However, the need to provide the user community with uncertainty values in the recommended data should also be stressed. Comprehensive cross-section and decay-data evaluations that include recommended data uncertainties are clearly merited to ensure the necessary quality and consistency of any data assembled in an appropriate database for nuclear medicine applications.

Requests for new nuclear data measurements are driven primarily by the results of methodical evaluations to identify inconsistencies and unforeseen gaps in the desired data. Thus, a healthy synergy exists in which $\alpha\beta\gamma$ spectroscopy laboratories undertake decay-data measurements driven by data inadequacies which have been highlighted by decay-scheme evaluations of direct relevance to nuclear medicine, the industrial and environmental business sectors, and basic nuclear physics research. Under these circumstances, the communication

and transfer of such data and information has improved considerably, and large quantities of nuclear data can be rapidly accessed within seconds, thanks to the work undertaken over many years by staff at the various national and international nuclear data centres. Thus, IAEA staff have created and maintain a dissemination system dedicated to nuclear data for medical applications. All of the recommended data that have evolved from the completed CRPs described above can be found on a dedicated IAEA Web site:

www-nds.iaea.org/medportal/

while all relevant interim IAEA INDC(NDS) reports are directly available from:

www-nds.iaea.org/publications/group_list.php?group=INDC-NDS

along with the final definitive IAEA technical reports for the two completed CRPs:

www-nds.iaea.org/publications/tecdocs/iaea-tecdoc-1211.pdf

www-nds.iaea.org/publications/tecdocs/technical-reports-series-473.pdf

Data Uncertainties

Data and their uncertainties are presented throughout the text and tables in the form 1234(x), where x is the uncertainty in the last digit or digits quoted in the measured or evaluated number. This uncertainty is generally expressed at the 1σ confidence level. Examples:

1739(8) means 1739 ± 8 ;

0.0171(22) means 0.0171 ± 0.0022 ; and

$1.13(17) \times 10^{+6}$ means $(1.13 \pm 0.17) \times 10^{+6}$.

Acknowledgements

Tibor Kibedi (Australian National University, Australia) and Filip Kondev (Argonne National Laboratory, USA) kindly provided the author with both technical and spectroscopic information, along with related presentational aids. The author would also like to thank staff within the IAEA Nuclear Data Section, and all co-workers associated with the various data development programmes for their assistance and contributions over many years, particularly participants in the relevant existing and completed IAEA coordinated research projects mentioned in this paper. Finally, he would like to acknowledge the considerable efforts of members of the International Network of Nuclear Structure and Decay Data Evaluators (ENSDF, custodian – NNDC, BNL, USA) and the Decay Data Evaluation Project (DDEP, custodian – LNHB, CEA Saclay, France) for their extensive, on-going contributions to the development and preparation of the decay databases described above.

References

1. G. Stöcklin, S.M. Qaim, F. Rösch, The impact of radioactivity on medicine, *Radiochim. Acta* **70/71** (1995) 249-272.
2. S.M. Qaim, Development of novel positron emitters for medical applications: nuclear and radiochemical aspects, *Radiochim. Acta* **99** (2011) 611-625.
3. S.M. Qaim, The present and future of medical radionuclide production, *Radiochim. Acta* **100** (2012) 635-651.
4. S.M. Qaim, Use of cyclotrons in medicine, *Radiat. Phys. Chem.* **71** (2004) 917-926.
5. S.M. Qaim, Cyclotron production of medical radionuclides, pp. 1903-1933 in *Handbook of Nuclear Chemistry*, Second Edition, Editors: A. Vértes, S. Nagy, Z. Klencsár, R.G. Lovas, F. Rösch, Vol. 4, Springer, Dordrecht, The Netherlands (2011).
6. K. Gul, A. Hermanne, M.G. Mustafa, F.M. Nortier, P. Obložinský, S.M. Qaim, B. Scholten, Yu.N. Shubin, S. Takács, F.T. Tárkányi, Zhuang Youxiang, Charged-particle cross-section database for medical radioisotope production: diagnostic radioisotopes

- and monitor reactions, *IAEA Report IAEA-TECDOC 1211*, May 2001, IAEA, Vienna, Austria;
also available from <http://www-nds.iaea.org/publications/tecdocs/iaea-tecdoc-1211.pdf>
7. E. Běták, A.D. Caldeira, R. Capote, B.V. Carlson, H.D. Choi, F.B. Guimarães, A.G. Ignatyuk, S.K. Kim, B. Kiraly, S.F. Kovalev, E. Menapace, A.L. Nichols, M. Nortier, P. Pompeia, S.M. Qaim, B. Scholten, Yu.N. Shubin, J.-Ch. Sublet, F. Tárkányi, Nuclear data for the production of therapeutic radionuclides, *IAEA Technical Reports Series No. 473*, December 2011, Editors: S.M. Qaim, F. Tárkányi and R. Capote, IAEA, Vienna, Austria, ISBN 978-92-0-115010-3;
also available from http://www-pub.iaea.org/MTCD/Publications/PDF/trs473_web.pdf
 8. R. Capote Noy, F.M. Nortier, Summary report of consultants' meeting on improvements in charged-particle monitor reactions and nuclear data for medical isotope production, 21-24 June 2011, IAEA Headquarters, *IAEA Report INDC(NDS)-0591*, September 2011, IAEA, Vienna, Austria;
also available from <http://www-nds.iaea.org/publications/indc/indc-nds-0591.pdf>
 9. R. Capote Noy, A.L. Nichols, Summary report of consultants' meeting on high-precision beta-intensity measurements and evaluations for specific PET radioisotopes, 3-5 September 2008, IAEA Headquarters, *IAEA Report INDC(NDS)-0535*, December 2008, IAEA, Vienna, Austria;
also available from <http://www-nds.iaea.org/publications/indc/indc-nds-0535.pdf>
 10. A.L. Nichols, S.M. Qaim, R. Capote Noy, Summary report of technical meeting on intermediate-term nuclear data needs for medical applications: cross sections and decay data, 22-26 August 2011, IAEA Headquarters, *IAEA Report INDC(NDS)-0596*, September 2011, IAEA, Vienna, Austria;
also available from <http://www-nds.iaea.org/publications/indc/indc-nds-0596.pdf>
 11. A.L. Nichols, R. Capote Noy, Summary report of first research coordination meeting on nuclear data for charged-particle monitor reactions and medical isotope production, 3-7 December 2012, IAEA Headquarters, *IAEA Report INDC(NDS)-0630*, February 2013, IAEA, Vienna, Austria;
also available from <http://www-nds.iaea.org/publications/indc/indc-nds-0630.pdf>
 12. J. Magill, J. Galy, *Radioactivity radionuclides radiation*, Springer, Berlin, Heidelberg and New York, 2005.
 13. A.L. Nichols, Decay data: review of measurements, evaluations and compilations, *Appl. Radiat. Isot.* **55** (2001) 23-70.
 14. A.L. Nichols, Nuclear decay data: on-going studies to address and improve radionuclide decay characteristics, invited paper published in *AIP Conf. Proc. - Int. Conf. on Nuclear Data for Science and Technology*, Editors: R.C. Haight, M.B. Chadwick, T. Kawano, P. Talou, Vol. 769, Part 1 (2005) 242-251, AIP, Melville, New York, USA, ISBN 0-7354-0254-X, ISSN 0094-243X.
 15. F. Szelecsényi, G.F. Steyn, Z. Kovács, C. Vermeulen, N.P. van der Meulen, S.G. Dolley, T.N. van der Walt, K. Suzuki, K. Mukai, Investigation of the $^{66}\text{Zn}(p,2p)^{64}\text{Cu}$ and $^{68}\text{Zn}(p,x)^{64}\text{Cu}$ nuclear processes up to 100 MeV: production of ^{64}Cu , *Nucl. Instrum. Methods Phys. Res.* **B240** (2005) 625-637.
 16. J.A. Nye, M.A. Avila-Rodriguez, R.J. Nickles, A new binary compound for the production of ^{124}I via the $^{124}\text{Te}(p,n)^{124}\text{I}$ reaction, *Appl. Radiat. Isot.* **65** (2007) 407-412.
 17. S.M. Qaim, T. Bisinger, K. Hilgers, D. Nayak, H.H. Coenen, Positron emission intensities in the decay of ^{64}Cu , ^{76}Br and ^{124}I , *Radiochim. Acta* **95** (2007) 67-73.
 18. R.J. Walen, V. Nedovessov, G. Bastin-Scoffier, Spectrographie α de ^{223}Ra (AcX) et de ses dérivés, *Nucl. Phys.* **35** (1962) 232-252.

19. B. Grennberg, A. Rytz, Absolute measurements of α -ray energies, *Metrologia* **7** (1971) 65-77.
20. E. Garcia-Toraño, Current status of alpha-particle spectrometry, *Appl. Radiat. Isot.* **64** (2006) 1273-1280.
21. F.G. Kondev, I. Ahmad, J.P. Greene, A.L. Nichols, M.A. Kellett, Measurements of absolute gamma-ray emission probabilities in the decay of ^{233}Pa , *Nucl. Instrum. Methods Phys. Res.* **A652** (2011) 654-656.
22. M.P. Croce, M.K. Bacrania, A.S. Hoover, M.W. Rabin, N.J. Hoteling, S.P. Lamont, A.A. Plionis, D.E. Dry, J.N. Ullom, D.A. Bennett, R.D. Horansky, V. Kotsubo, R. Cantor, Cryogenic microcalorimeter system for ultra-high resolution alpha-particle spectrometry, published in *AIP Conf. Proc. – 13th Int. Workshop on Low Temperature Detectors*, Editors: B. Cabrera, A. Miller, B. Young, Vol. 1185 (2009) 741-744, AIP, Melville, New York, USA, ISBN 0-7354-0751-0/09.
23. P.C. Ranitzsch, S. Kempf, A. Pabinger, C. Pies, J.-P. Porst, S. Schäfer, A. Fleischmann, L. Gastaldo, C. Enss, Y.S. Jang, I.H. Kim, M.S. Kim, Y.H. Kim, J.S. Lee, K.B. Lee, M.K. Lee, S.J. Lee, W.S. Yoon, Y.N. Yuryev, Development of cryogenic alpha spectrometers using metallic magnetic calorimeters, *Nucl. Instrum. Methods Phys. Res.* **A652** (2011) 299-301.
24. I.Y. Lee, M.A. Deleplanque, K. Vetter, Developments in large gamma-ray detector arrays, *Rep. Prog. Phys.* **66** (2003) 1095-1144.
25. J. Eberth, J. Simpson, From Ge(Li) detectors to gamma-ray tracking arrays – 50 years of gamma spectroscopy with germanium detectors, *Prog. Part. Nucl. Phys.* **60** (2008) 283-337.
26. K. Korten, S. Lunardi (Editors), Achievements with the Euroball spectrometer, 1997-2003 – http://www.lnl.infn.it/~annrep/other_reports/euroball/eb_index.htm
27. Gammasphere – <http://www.physics.fsu.edu/GS10Yr/introduction.htm>
28. S. Akkoyun, A. Algora, B. Alikhani, *et al.*, AGATA – Advanced GAMMA Tracking Array, *Nucl. Instrum. Methods Phys. Res.* **A668** (2012) 26-58.
29. I.Y. Lee, Gamma-ray tracking detectors: physics opportunities and status of GRETINA, *Nucl. Phys.* **A834** (2010) 743c-746c.
30. A. Gadea, E. Farnea, J.J. Valiente-Dobón, *et al.*, Conceptual design and infrastructure for the installation of the first AGATA sub-array at LNL, *Nucl. Instrum. Methods Phys. Res.* **A654** (2011) 88-96.
31. E.V.D. van Loef, P. Dorenbos, C.W.E. van Eijk, K. Krämer, H.U. Güdel, High-energy-resolution scintillator: Ce^{3+} activated LaCl_3 , *Appl. Phys. Lett.* **77** (2000) 1467-1468.
32. E.V.D. van Loef, P. Dorenbos, C.W.E. van Eijk, K. Krämer, H.U. Güdel, High-energy-resolution scintillator: Ce^{3+} activated LaBr_3 , *Appl. Phys. Lett.* **79** (2001) 1573-1575.
33. J. Glodo, W.W. Moses, W.M. Higgins, E.V.D. van Loef, P. Wong, S.E. Derenzo, M.J. Weber, K.S. Shah, Effects of Ce concentration on scintillation properties of $\text{LaBr}_3:\text{Ce}$, *IEEE Trans. Nucl. Sci.* **52** (2005) 1805-1808.
34. S. Zhu, F.G. Kondev, M.P. Carpenter, I. Ahmad, C.J. Chiara, J.P. Greene, G. Gurdal, R.V.F. Janssens, S. Lalkovski, T. Lauritsen, D. Seweryniak, γ -ray coincidence and fast-timing measurements using $\text{LaBr}_3(\text{Ce})$ detectors and Gammasphere, *Nucl. Instrum. Methods Phys. Res.* **A652** (2011) 231-233.
35. N.J. Cherepy, S.A. Payne, S.J. Asztalos, *et al.*, Scintillators with potential to supersede lanthanum bromide, *IEEE Trans. Nucl. Sci.* **56** (2009) 873-880.
36. C.K. Stahle, C.A. Allen, K.R. Boyce, *et al.*, The next-generation microcalorimeter array of XRS on Astro-E2, *Nucl. Instrum. Methods Phys. Res.* **A520** (2004) 466-468.
37. F.S. Porter, G.V. Brown, K.R. Boyce, R.L. Kelley, C.A. Kilbourne, P. Beiersdorfer, Hui Chen, S. Terracol, S.M. Kahn, A.E. Szymkowiak, The Astro-E2 X-ray

- spectrometer/EBIT microcalorimeter X-ray spectrometer, *Rev. Sci. Instrum.* **75** (2004) 3772-3774.
38. B.R. Beck, J.A. Becker, P. Beiersdorfer, G.V. Brown, K.J. Moody, J.B. Wilhelmy, F.S. Porter, C.A. Kilbourne, R.L. Kelley, Energy splitting of the ground-state doublet in the nucleus ^{229}Th , *Phys. Rev. Lett.* **98** (2007) 142501, 1-4.
 39. K.M. Bisgård, P. Dahl, K. Olesen, Multipolarities of U^{233} transitions, *Nucl. Phys.* **12** (1959) 612-618.
 40. R.G. Albridge, J.M. Hollander, C.J. Gallagher, J.H. Hamilton, The energy levels of U^{233} , *Nucl. Phys.* **27** (1961) 529-553.
 41. S.A. Woods, P. Christmas, P. Cross, S.M. Judge, W. Gelletly, Decay studies of ^{237}Np with an iron-free $\pi\sqrt{2}$ double-focusing β -ray spectrometer of improved efficiency, *Nucl. Instrum. Methods Phys. Res.* **A264** (1988) 333-356.
 42. Ch. Briançon, B. Legrand, R.J. Walen, Ts. Vylov, A. Minkova, A. Inoyatov, A new combined electrostatic electron spectrometer, *Nucl. Instrum. Methods Phys. Res.* **221** (1984) 547-557.
 43. A. Kovalík, E.A. Yakushev, D.V. Filosofov, V.M. Gorozhankin, P.A. Petev, M.A. Mahmoud, Precise measurement of the KLL and KLX Auger spectra of cadmium from the EC-decay of ^{111}In , *J. Electron Spectrosc. Relat. Phenom.* **105** (1999) 219-229.
 44. E.A. Yakushev, A. Kovalík, D.V. Filosofov, N.A. Korolev, N.A. Lebedev, A.V. Lubashevski, F. Rösch, A.F. Novgorodov, *Appl. Radiat. Isot.* **62** (2005) 451-456.
 45. A. Inoyatov, A.V. Lubashevsky, A. Kovalík, E.A. Yakushev, D.V. Filosofov, Yu.S. Borodin, V.M. Gorozhankin, A.F. Novgorodov, Ts. Vylov, V.S. Zhdanov, A detailed experimental investigation of the KMM + KMN + KNN Auger electron spectrum of ^{111}Cd from the EC-decay of ^{111}In , *J. Electron Spectrosc. Relat. Phenom.* **151** (2006) 193-198.
 46. M. Gierlik, A. Płochocki, M. Karny, *et al.*, Gamow-Teller strength distribution near ^{100}Sn – the beta decay of ^{102}In , *Nucl. Phys.* **A724** (2003) 313-332.
 47. E. Poirier, F. Maréchal, Ph. Dessagne, *et al.*, B(GT) strength from β -decay measurements and inferred shape mixing in ^{74}Kr , *Phys. Rev.* **C69** (2004) 034307, 1-8.
 48. K. Way, Nuclear data: a collection of experimental values of half-lives, radiation energies, relative isotopic abundances, nuclear moments and cross sections compiled by the National Bureau of Standards nuclear data group, NBS circular no. 499 (1950), National Bureau of Standards, US Department of Commerce, Washington DC, USA.
 49. Evaluated Nuclear Structure Data File, National Nuclear Data Center, Brookhaven National Laboratory, Upton, New York, USA; also *Nuclear Data Sheets*, Elsevier Inc., Amsterdam, the Netherlands, and <http://www.nndc.bnl.gov/ensdf/>
 50. A.L. Nichols, J.K. Tuli, The aims and activities of the International Network of Nuclear Structure and Decay Data Evaluators, invited paper published in *Proc. Int. Conf. on Nuclear Data for Science and Technology*, Editors: O. Bersillon, F. Gunsing, E. Bauge, R. Jacqmin, S. Leray, Vol. 1 (2008) 37-42, EDP Sciences, Les Ulis, France, ISBN 978-2-7598-0090-2.
 51. J.K. Tuli, *Nuclear wallet cards*, October 2011, Brookhaven National Laboratory, Upton, New York, USA.
 52. M.-M. Bé, V. Chisté, C. Dulieu, E. Browne, V. Chechev, N. Kuzmenko, R. Helmer, A. Nichols, E. Schönfeld, R. Dersch, Table of radionuclides (Vol. 1 – A = 1 to 150), *Monographie BIPM-5*, Bureau International des Poids et Mesures, Sèvres, France (2004), ISBN 92-822-2206-3; also available from http://www.bipm.org/utils/common/pdf/monographieRI/Monographie_BIPM-5_Tables_Vol1.pdf
 53. M.-M. Bé, V. Chisté, C. Dulieu, E. Browne, V. Chechev, N. Kuzmenko, R. Helmer, A. Nichols, E. Schönfeld, R. Dersch, Table of radionuclides (Vol. 2 – A = 151 to 242),

- Monographie BIPM-5*, Bureau International des Poids et Mesures, Sèvres, France (2004), ISBN 92-822-2207-1; also available from http://www.bipm.org/utis/common/pdf/monographieRI/Monographie_BIPM-5_Tables_Vol2.pdf
54. M.-M. Bé, V. Chisté, C. Dulieu, E. Browne, C. Baglin, V. Chechev, N. Kuzmenko, R. Helmer, F. Kondev, D. MacMahon, K.B. Lee, Table of radionuclides (Vol. 3 – A = 3 to 244), *Monographie BIPM-5*, Bureau International des Poids et Mesures, Sèvres, France (2006), ISBN 92-822-2218-7; also available from http://www.bipm.org/utis/common/pdf/monographieRI/Monographie_BIPM-5_Tables_Vol3.pdf
 55. M.-M. Bé, V. Chisté, C. Dulieu, E. Browne, V. Chechev, N. Kuzmenko, F. Kondev, A. Luca, M. Galán, A. Pearce, X. Huang, Table of radionuclides (Vol. 4 – A = 133 to 252), *Monographie BIPM-5*, Bureau International des Poids et Mesures, Sèvres, France (2008), ISBN 92-822-2230-6; also available from http://www.bipm.org/utis/common/pdf/monographieRI/Monographie_BIPM-5_Tables_Vol4.pdf
 56. M.-M. Bé, V. Chisté, C. Dulieu, X. Mougeot, E. Browne, V. Chechev, N. Kuzmenko, F. Kondev, A. Luca, M. Galán, A.L. Nichols, A. Arinc, X. Huang, Table of radionuclides (Vol. 5 – A = 22 to 244), *Monographie BIPM-5*, Bureau International des Poids et Mesures, Sèvres, France (2010), ISBN-13 978-92-822-2234-8; also available from http://www.bipm.org/utis/common/pdf/monographieRI/Monographie_BIPM-5_Tables_Vol5.pdf
 57. M.-M. Bé, V. Chisté, C. Dulieu, X. Mougeot, V.P. Chechev, N.K. Kuzmenko, F.G. Kondev, A. Luca, M. Galán, A.L. Nichols, A. Arinc, A. Pearce, X. Huang, B. Wang, Table of radionuclides (Vol. 6 – A = 22 to 242), *Monographie BIPM-5*, Bureau International des Poids et Mesures, Sèvres, France (2011), ISBN-13 978-92-822-2242-3; also available from http://www.bipm.org/utis/common/pdf/monographieRI/Monographie_BIPM-5_Tables_Vol6.pdf
 58. M.-M. Bé, V. Chisté, C. Dulieu, X. Mougeot, V.P. Chechev, F.G. Kondev, A.L. Nichols, X. Huang, B. Wang, Table of radionuclides (Vol. 7 – A = 14 to 245), *Monographie BIPM-5*, Bureau International des Poids et Mesures, Sèvres, France (2013), ISBN-13 978-92-822-2248-5; also available from http://www.bipm.org/utis/common/pdf/monographieRI/Monographie_BIPM-5_Tables_Vol7.pdf
 59. M.-M. Bé, V. Chisté, C. Dulieu, X. Mougeot, E. Browne, C. Baglin, V.P. Chechev, A. Egorov, N.K. Kuzmenko, V.O. Sergeev, F.G. Kondev, A. Luca, M. Galán, X. Huang, B. Wang, R.G. Helmer, E. Schönfeld, R. Dersch, V.R. Vanin, R.M. de Castro, A.L. Nichols, T.D. MacMahon, A. Pearce, A. Arinc, K.B. Lee, S.C. Wu, Table of radionuclides, comments on evaluations (Vols. 1 – 7), *Monographie BIPM-5* (2013) Bureau International des Poids et Mesures, France; also available from http://www.bipm.org/utis/common/pdf/monographieRI/Monographie_BIPM-5_Comments_Vol1-7.pdf
 60. A.L. Nichols, IAEA Co-ordinated Research Project: update of X-ray and gamma-ray decay data standards for detector calibration and other applications, *Appl. Radiat. Isot.* **60** (2004) 247-256.
 61. M.-M. Bé, V.P. Chechev, R. Dersch, O.A.M. Helene, R.G. Helmer, M. Herman, S. Hlaváč, A. Marcinkowski, G.L. Molnár, A.L. Nichols, E. Schönfeld, V.R. Vanin, M.J. Woods, Update of X ray and gamma ray decay data standards for detector calibration and other applications, Volume 1: Recommended decay data, high energy gamma ray standards and angular correlation coefficients, *IAEA Scientific and Technical Report STI/PUB/1287*, May 2007, International Atomic Energy Agency, Vienna, Austria, ISBN 92-0-113606-4; also available from http://www-nds.iaea.org/publications/tecdocs/sti-pub-1287_Voll.pdf
 62. M.-M. Bé, V.P. Chechev, R. Dersch, O.A.M. Helene, R.G. Helmer, M. Herman, S. Hlaváč, A. Marcinkowski, G.L. Molnár, A.L. Nichols, E. Schönfeld, V.R. Vanin, M.J. Woods, Update of X ray and gamma ray decay data standards for detector calibration and other applications, Volume 2: Data selection, assessment and evaluation

- procedures, *IAEA Scientific and Technical Report STI/PUB/1287*, May 2007, International Atomic Energy Agency, Vienna, Austria, ISBN 92-0-113606-4; also available from http://www-nds.iaea.org/publications/tecdocs/sti-pub-1287_Vol2.pdf
63. M.A. Kellett, F.G. Kondev, A.L. Nichols, IAEA coordinated research project: updated decay data library for actinides, *Appl. Radiat. Isot.* **66** (2008) 694-700.
 64. M.A. Kellett, M.-M. Bé, V. Chechev, X. Huang, F.G. Kondev, A. Luca, G. Mukherjee, A.L. Nichols, A. Pearce, New IAEA actinide decay data library, *J. Korean Phys. Soc. – Proc. Int. Conf. on Nuclear Data for Science and Technology*, **59**, No. 2 (2011) 1455-1460, Korean Physical Society, South Korea.
 65. M.A. Kellett, Assessment of actinide decay data evaluations: findings of an IAEA coordinated research project, *Appl. Radiat. Isot.* **70** (2012) 1919-1923.
 66. M.-M. Bé, V.P. Chechev, X. Huang, M.A. Kellett, F.G. Kondev, A. Luca, G. Mukherjee, A.L. Nichols, A.K. Pearce, *Updated decay data library for actinides*, IAEA technical report in preparation.
 67. R.L. Heath, *Gamma-ray spectrum catalogue*, AEC report ANC-1000-2, 1974.
 68. R.G. Helmer, R.J. Gehrke, J.R. Davidson, J.W. Mandler, Scientists, spectrometry and gamma-ray spectrum catalogues, 1957-2007, *J. Radioanal. Nucl. Chem.* **243** (2000) 109-117.
 69. S.M. Qaim, Nuclear data for medical applications: an overview, *Radiochim. Acta* **89** (2001) 189-196.
 70. S.M. Qaim, Nuclear data relevant to the production and application of diagnostic radionuclides, *Radiochim. Acta* **89** (2001) 223-232.
 71. S.M. Qaim, Therapeutic radionuclides and nuclear data, *Radiochim. Acta* **89** (2001) 297-302.
 72. T.W. Burrows, The program RADLST, *Brookhaven National Laboratory Report BNL-NCS-52142*, February 1988; also available from http://www.nndc.bnl.gov/nndcscr/ensdf_pgm/analysis/radlst/radlstdoc.pdf

Figure captions

1. Alpha-particle spectra of thin mass-separated sources of (a) ^{237}Np , and (b) ^{243}Am measured by means of a 450-mm² passivated implanted planar silicon (PIPS) detector – main α peaks are labelled in keV energy units [21].
2. ^{67}Cu β^- decay: Gamma-ray (HPGe detector) and electron spectra (1mm thick Si detector).
3. Gamma-ray spectrum of a chemically-purified ^{233}Pa source measured by means of a 2-cm² x 1-cm planar low-energy photon spectrometer (LEPS), at a source-to-detector distance of 5 cm – main γ peaks are labelled in keV energy units [21].
4. Half of the modular layout of HPGe detectors for (a) Gammasphere, and (b) Euroball.
5. Module-detector/configurations: (a) full 4π solid-angle arrangement for GRETA, and (b) partial cross-sectional arrangement for AGATA.
6. Quarter-based layout of the GRETINA detectors (foreground) compared with the full 4π solid-angle system designed for GRETA (background).
7. KLL-Auger spectrum of ^{111}Cd from the EC decay of ^{111}In measured at 7-eV resolution and 2-eV step size; spectral components are shown as continuous lines [43].
8. KMM-, KMN- and KNN-Auger spectrum of ^{111}Cd from the EC decay of ^{111}In measured at 21-eV resolution and 2-eV step size; spectral components are shown as continuous lines [45].
9. Nuclear data sheets for the EC decay of ^{62}Cu (ENSDF [49]).
10. Nuclear data sheets for the IT decay of $^{99}\text{Tc}^m$ (ENSDF [49]).

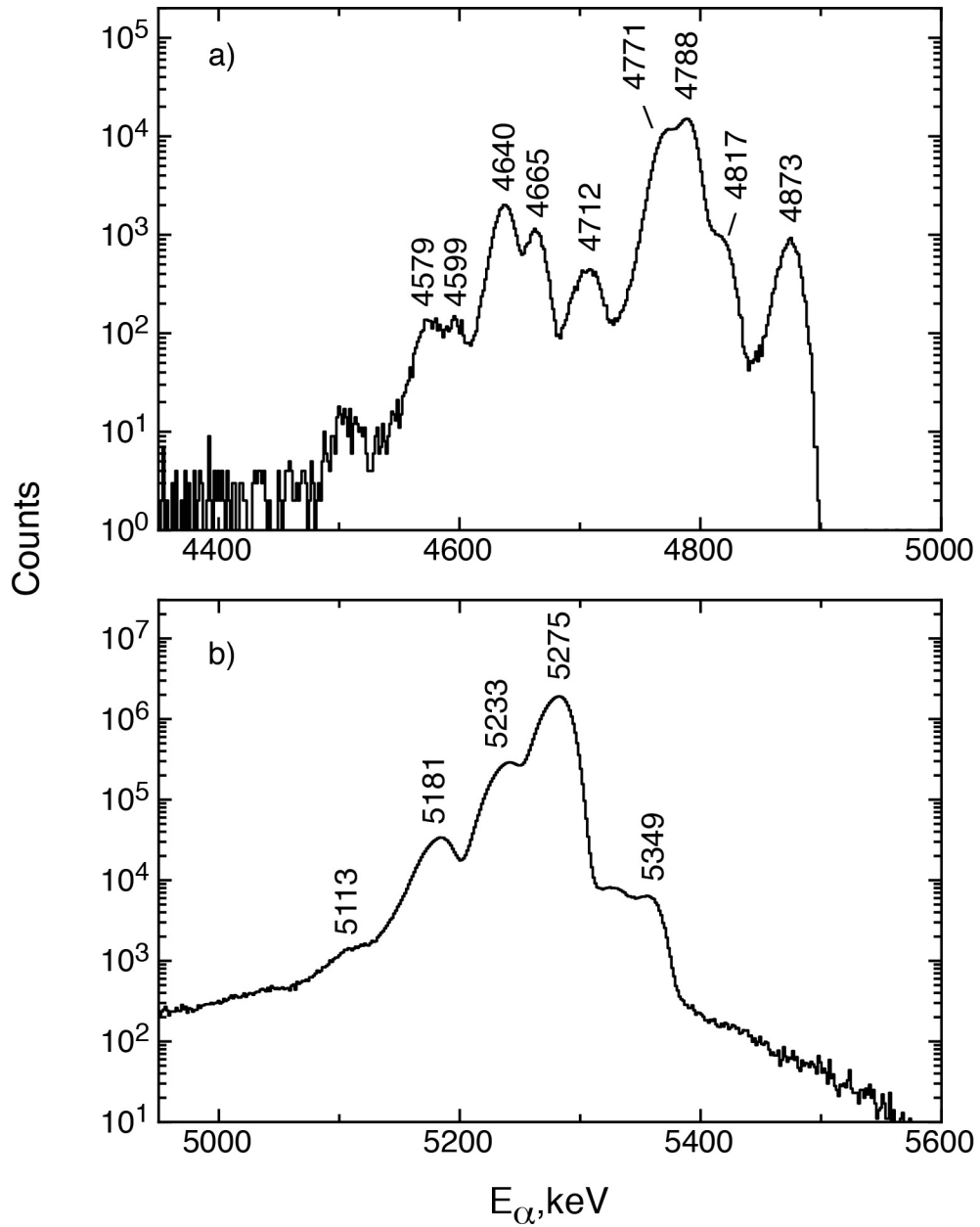


Fig. 1 Alpha-particle spectra of thin mass-separated sources of (a) ^{237}Np , and (b) ^{243}Am measured by means of a 450-mm² passivated implanted planar silicon (PIPS) detector – main α peaks are labelled in keV energy units [21].

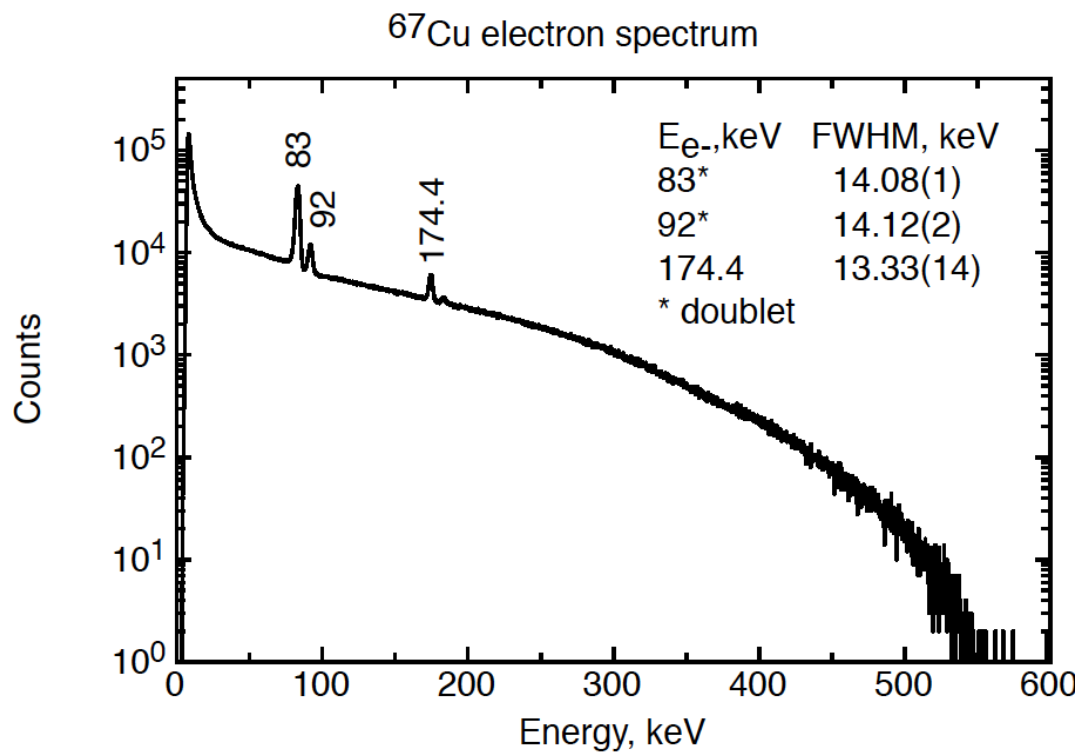
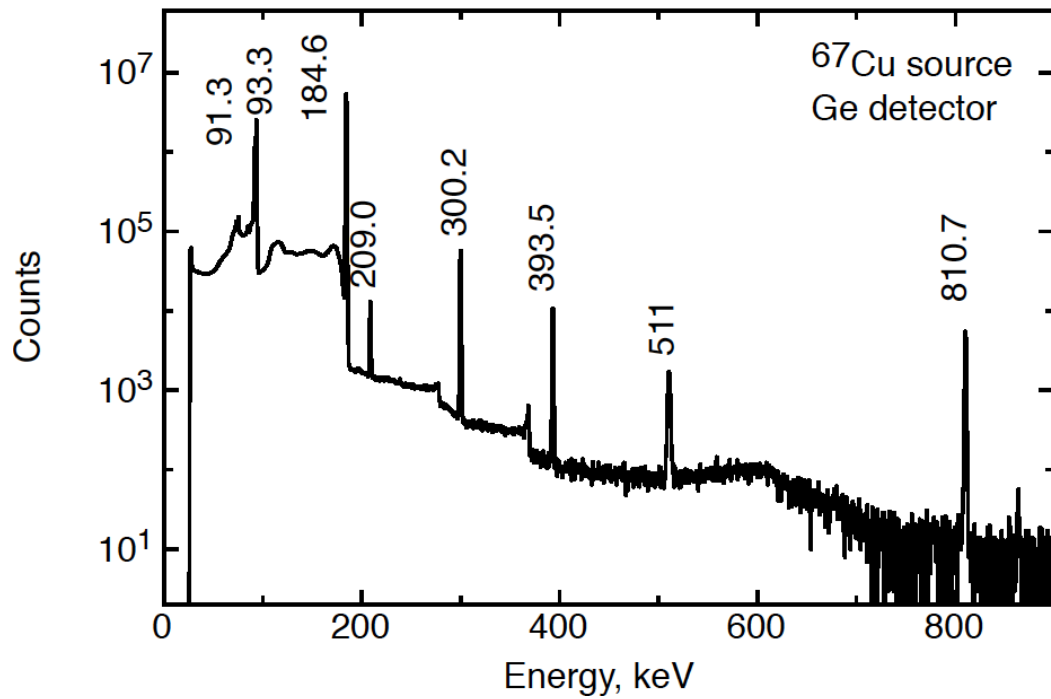


Fig. 2. ^{67}Cu β^- decay: Gamma-ray (HPGe detector) and electron spectra (1mm thick Si detector).

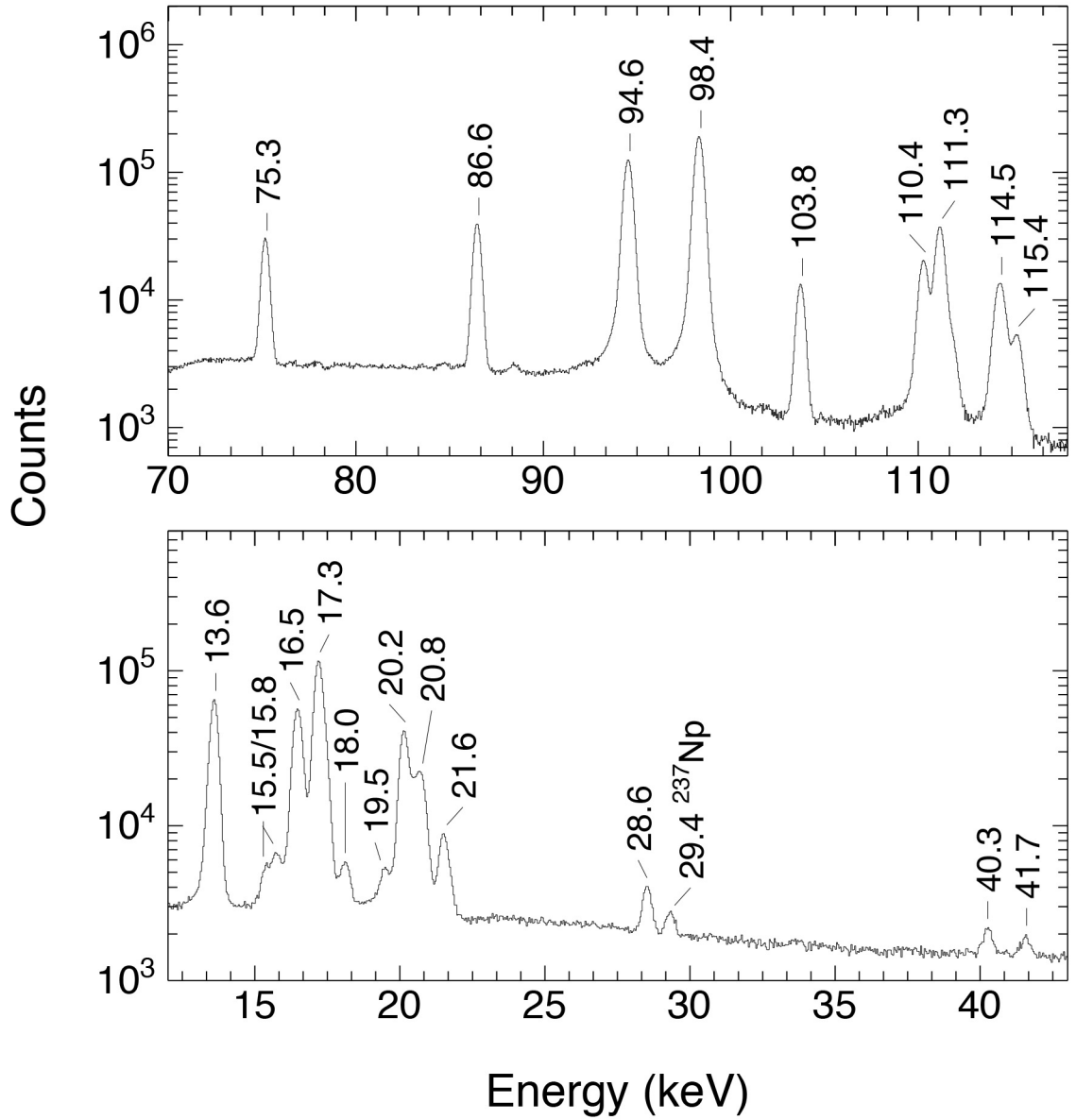
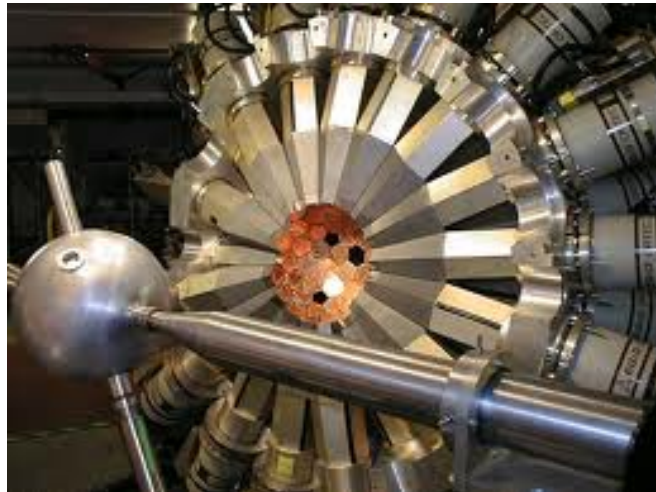
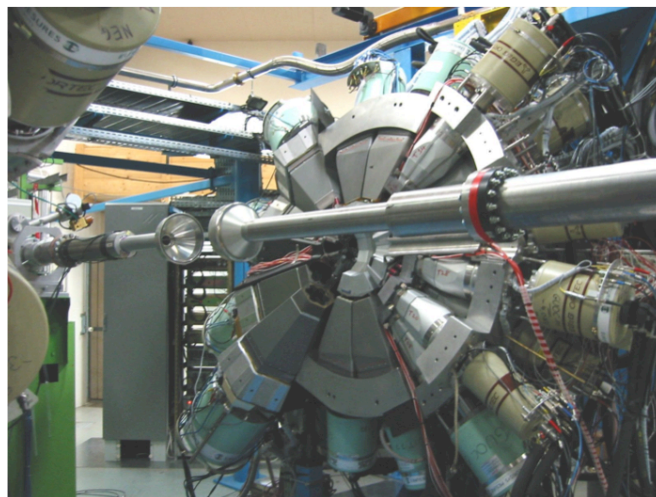


Fig. 3. Gamma-ray spectrum of a chemically-purified ^{233}Pa source measured by means of a $2\text{-cm}^2 \times 1\text{-cm}$ planar low-energy photon spectrometer (LEPS), at a source-to-detector distance of 5 cm – main γ peaks are labelled in keV energy units [21].

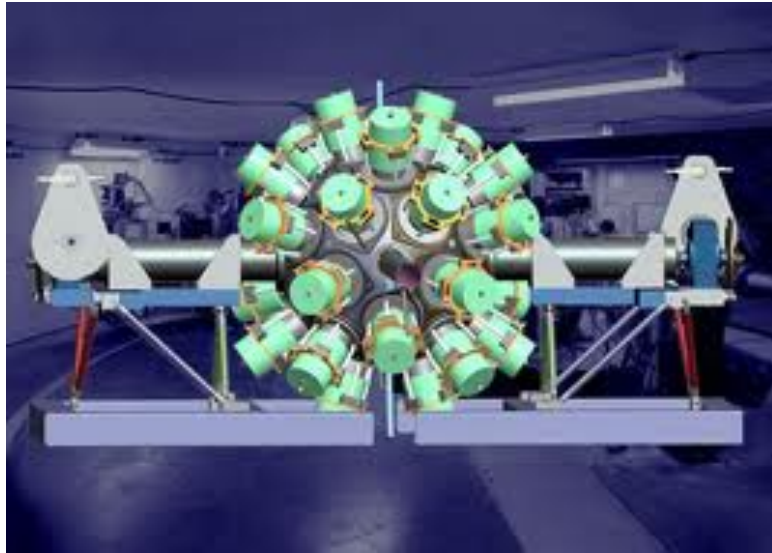


(a)

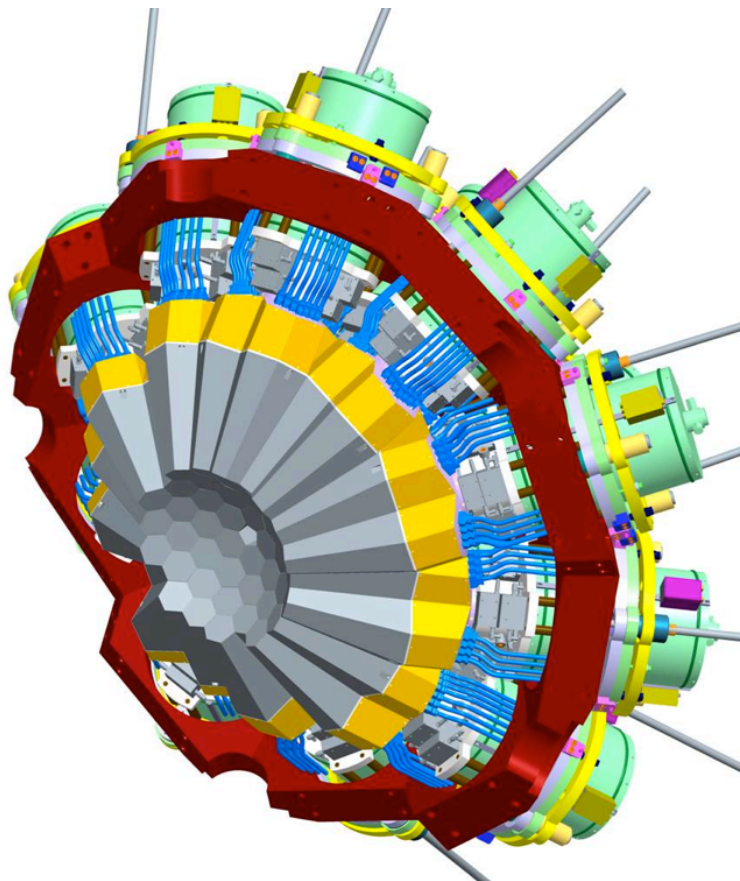


(b)

Fig. 4. Half of the modular layout of HPGe detectors for (a) Gammasphere, and (b) Euroball.



(a)



(b)

Fig. 5. Module-detector/configurations: (a) full 4π solid-angle arrangement for GRETA, and (b) partial cross-sectional arrangement for AGATA.

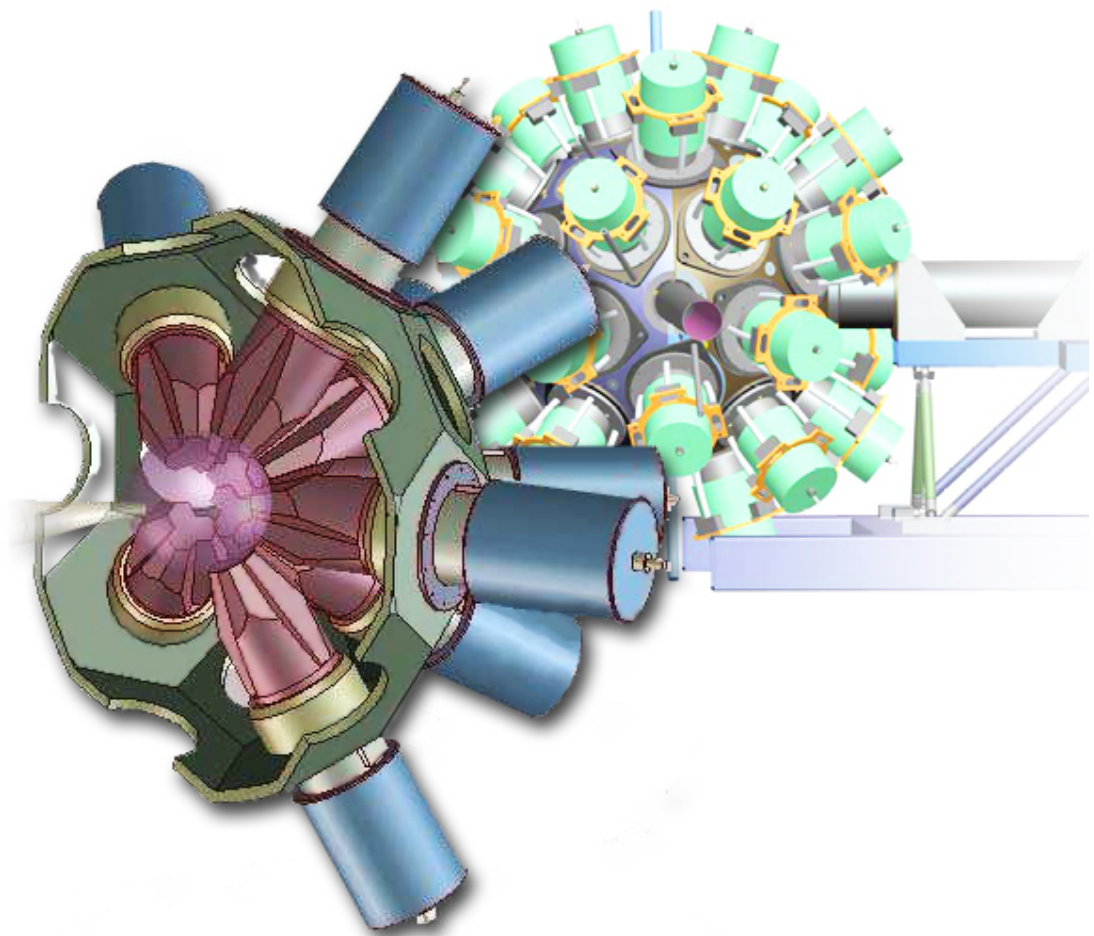


Fig. 6. Quarter-based layout of the GREY detectors (foreground) compared with the full 4π solid-angle system proposed for GRETA (background).

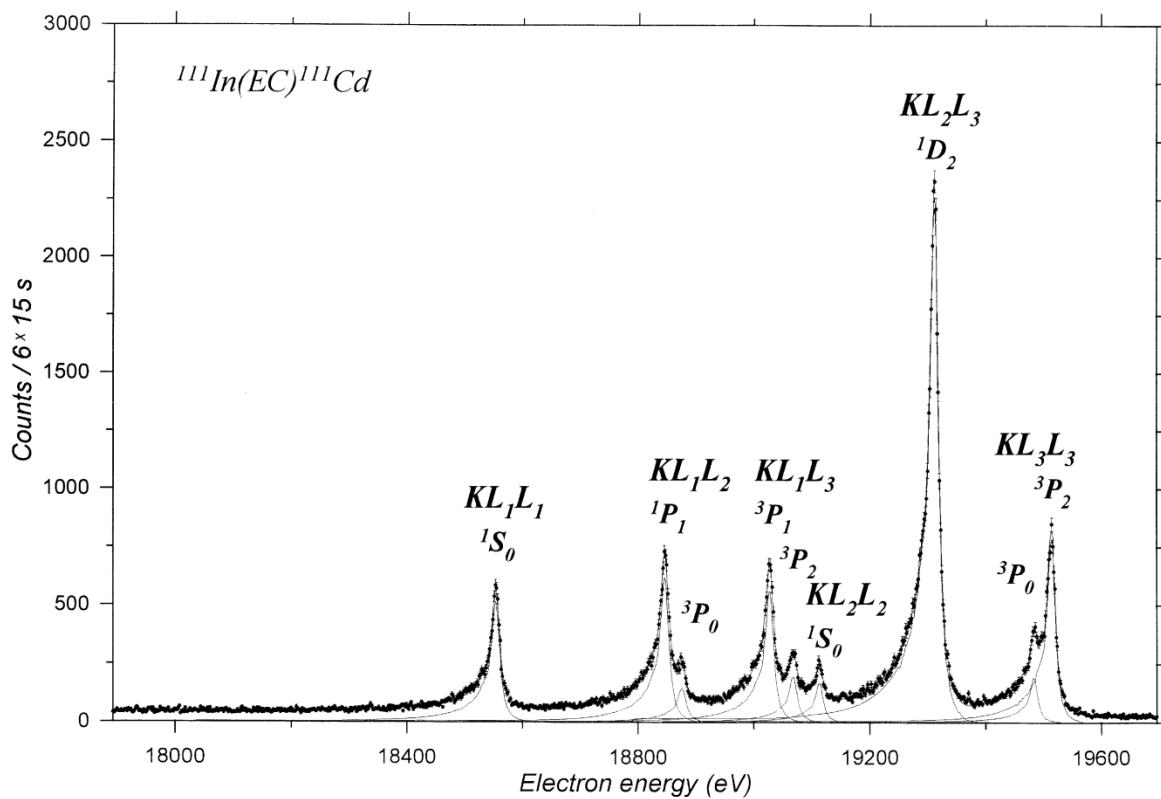


Fig. 7. KLL-Auger spectrum of ^{111}Cd from the EC decay of ^{111}In measured at 7-eV resolution and 2-eV step size; spectral components are shown as continuous lines [43].

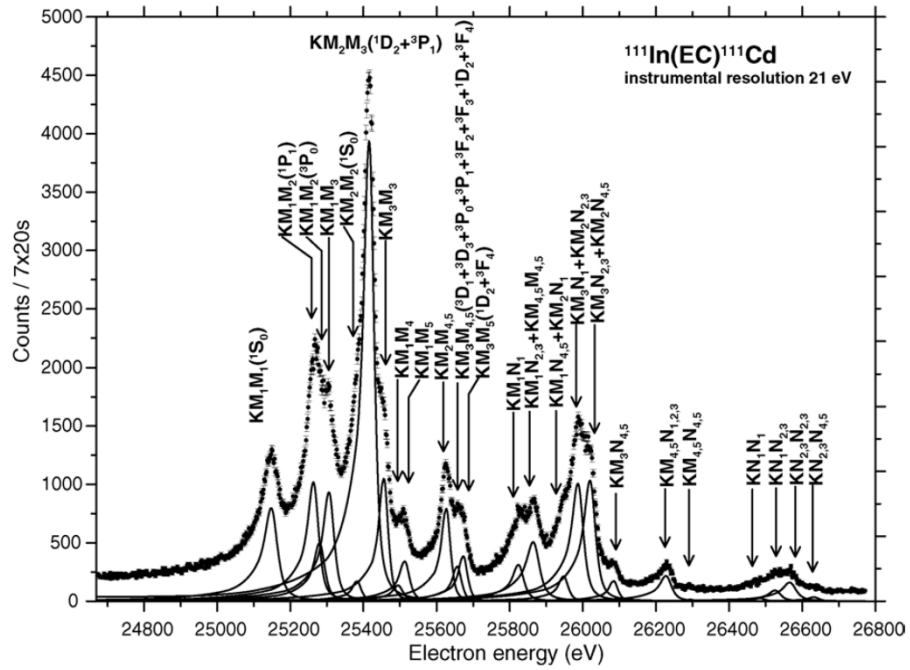


Fig. 8. KMM-, KMN- and KNN-Auger spectrum of ^{111}Cd from the EC decay of ^{111}In measured at 21-eV resolution and 2-eV step size; spectral components are shown as continuous lines [45].

Fig. 9. Nuclear data sheets for the EC decay of ^{62}Cu (ENSDF[49])

$^{62}\text{Ni}_{34}$
 $^{28}\text{Ni}_{34}$

$^{62}\text{Ni}_{34}$
 $^{28}\text{Ni}_{34}$

^{62}Cu ϵ Decay (9.67 min) 1971JoZN,1975Ca40,1970Va11

Parent ^{62}Cu : $E=0.0$; $J\pi=1+$; $T_{1/2}=9.67$ min 3; $Q(\text{g.s.})=3958.90$ 48; $\% \epsilon + \% \beta^+$ decay=100.
 ^{62}Cu -J: From Adopted Levels of ^{62}Cu .
 ^{62}Cu -Q(ϵ): From 2011AuZZ. 2003Au03 give 3948 4.
 ^{62}Cu - $T_{1/2}$: weighted average of two sets of data from 1997Zi06 (also 2002Un02). Others: 10.5 min 5 (1937He05, also Nature 138, 723 (1936); Physica 4, 160 (1937)); 10.5 min 3 (1937Bo10), 10.0 min 1 (1937Ri01), 9.92 min 5 (1939Cr03), 10.1 min 1 (1947Le07), 9.88 min (1948Wa13), 9.9 min (1948Pe03), 9.80 min 7 (1951Go43), 9.8 min (1952Ma28), 9.73 min 2 (1954Be84), 10.1 min 2 (1954Nu27), 9.94 min 4 (1958Po07), 9.90 min 4 (1961Sa19), 9.76 min 2 (1965Eb01), 9.79 min 6 (1965Li11), 9.7 min (1966Ch24), 9.7 min 1 (1969Bo11), 9.73 min 2 (1969Jo07), 9.80 min 2 (1975Ca40). Weighted average of all data listed with quantified uncertainties is 9.76 min 2, but with reduced $\chi^2=2.5$ to 5.4 depending on which method is used. LWM gives 9.90 min 17 in order to include the most precise value.
 1971JoZN, 1969Jo07 (thesis): source from $^{62}\text{Ni}(p,n)$ at 7, 13 MeV and from decay of ^{62}Zn parent. Measured $E\gamma$, $I\gamma$, and conversion electrons using a double-focusing magnetic spectrometer. 1969Jo07 report four gamma rays and intensity of 511 annihilation radiation, but the latter is revised in 1971JoZN. More details can be found in the thesis (1971JoZN).
 1975Ca40: source from $^{63}\text{Cu}(n,2n)$ at 14 MeV. Measured $E\gamma$, $I\gamma$ for seven γ rays.
 1970Va11: source from $^{62}\text{Ni}(p,n)$ at 6.8 MeV; measured $E\gamma$, $I\gamma$ for nine γ rays.
 1969Es03: source from ^{62}Zn parent produced in $\text{Cu}(p,2n)$; measured $E\gamma$, $I\gamma$ for five γ rays.
 Others:
 1993Os06 (also 2001Ko07): measured β^+ spectrum, deduced maximum $E\beta$, and $Q(\epsilon)=3967$ 16.
 1976Ca31: measured $\gamma\gamma(\theta)$ using $\text{Ge}(\text{Li})$ and $\text{NaI}(\text{Tl})$ detectors; deduced $E2/M1$ mixing ratio for second $2+$ to first $2+$ transition.
 1967An01: source from ^{62}Zn parent produced in $\text{Cu}(p,2n)$; measured β^+ spectrum by a double-focusing iron yoke β spectrometer; deduced $E\beta(\text{max})=2934$ 7.
 1964Sa32: source from ^{62}Zn parent produced in $\text{Cu}(p,2n)$. Measured β^+ and ce spectra using double-focusing β spectrometer.
 1954Nu27: source from ^{62}Zn parent produced in $\text{Cu}(d,3n)$. Measured upper limit of γ intensity of $<5\%$ relative to total β^+ emission for 350–650 keV region, and $<3\%$ for higher-energy region. Deduced $E\beta(\text{max})=2910$ 10.
 Half-life measurements of ^{62}Cu g.s.: 2002Un02, 1997Zi06, 1975Ca40, 1969Jo07, 1969Bo11, 1966Ch24, 1965Li11, 1965Eb01, 1961Sa19, 1958Po07, 1954Nu27, 1954Be84, 1952Ma28, 1951Go43, 1947Le07, 1939Cr03.
 Production and identification of ^{62}Cu isotope: 1937Ri01, 1937He05, 1937Bo10, 1938St05, 1946Me01, 1950Gh62, 1950Ha65, 1954Nu27.
 β measurements: 1949Be17, 1950Ha65, 1954Nu27, 1958Cr86, 1964Sa32, 1967An01.
 $\beta\gamma$ coin: 1958Cr86 (1750 β –1173 γ coin).
 Other γ -ray measurements: 1955Re08, 1957Br20, 1958Bu10.

^{62}Ni Levels

E(level) [†]	$J\pi$ [‡]	Comments
0.0	0+	
1172.97 10	2+	
2048.63 12	0+	$J\pi$: from $\gamma\gamma(\theta)$ (1976Ca31).
2301.95 8	2+	
2890.6 4	0+	
3158.1 10	2+	
3257.7 4	2+	
3270.9 3	1+, 2+	
3370.2 3	1+, 2+	
3861.7 11	1+, 2+	

[†] From least-squares fit to $E\gamma$ data.

[‡] From Adopted Levels.

β^+, ϵ Data

$E\epsilon$	E(level)	$I\beta^+$ [†]	$I\epsilon$ [†]	Log ft	$I(\epsilon + \beta^+)$ [†]	Comments
(97.2 12)	3861.7		0.00037 7	5.60 9		$\epsilon K=0.8711$ 3; $\epsilon L=0.11001$ 25; $\epsilon M+=0.01891$ 5.
(588.7 6)	3370.2		0.0128 17	5.69 6		$\epsilon K=0.8856$; $\epsilon L=0.09788$; $\epsilon M+=0.01657$.
(688.0 6)	3270.9		0.0058 5	6.17 4		$\epsilon K=0.8859$; $\epsilon L=0.09756$; $\epsilon M+=0.01651$.
(701.2 7)	3257.7		0.0049 10	6.26 9		$\epsilon K=0.8860$; $\epsilon L=0.09753$; $\epsilon M+=0.01650$.
(800.8 11)	3158.1		0.0018 4	6.81 10		$\epsilon K=0.8862$; $\epsilon L=0.09730$; $\epsilon M+=0.01646$.
(1068.3 7)	2890.6		0.0006 3	7.54 22		$\epsilon K=0.8867$; $\epsilon L=0.09690$; $\epsilon M+=0.01638$.
(1656.9 5)	2301.95	0.019 1	0.053 2	5.98 2	0.072 3	av $E\beta=270.5$ 4; $\epsilon K=0.6497$ 10; $\epsilon L=0.07066$ 11; $\epsilon M+=0.01194$ 2.

Continued on next page (footnotes at end of table)

⁶²Cu ϵ Decay (9.67 min) 1971JoZN,1975Ca40,1970Va11 (continued)

β^+, ϵ Data (continued)

E ϵ	E(level)	I β^+ †	I ϵ †	Log ft	I($\epsilon+\beta^+$)†	Comments
(1910.3 5)	2048.63	0.076 4	0.066 3	6.00 2	0.142 7	E ϵ : E β^+ (max)=870 10 (1964Sa32). av E β =379.6 4; ϵ K=0.4148 9; ϵ L=0.04505 9; ϵ M+=0.00761 2.
(2785.9 5)	1172.97	0.138 6	0.013 1	7.03 2	0.151 7	av E β =772.1 5; ϵ K=0.07888 13; ϵ L=0.00855 2; ϵ M+=0.001443 1.
(3958.9 5)	0.0	97.599 25	2.009 20	5.158 2	99.608 24	E ϵ : E β^+ (max)=1750 10 (1964Sa32), I β =1.8%. av E β =1320.7 5; ϵ K=0.01790 2; ϵ L=0.0019367 2; ϵ M+=0.000327 1. E ϵ : E β^+ (max)=2945 16 (2001Ko07,1993Os06), 2934 7 (1967An01), 2923 7 (1964Sa32), 2910 10 (1954Nu27). I($\epsilon+\beta^+$): 100-(feeding to excited states). Other: I β =93.9% (1964Sa32).

† Absolute intensity per 100 decays.

γ (⁶²Ni)

Measured intensity of γ^+ annihilation radiation: 58100 30 (1971JoZN), 55900 34 (1970Va11), 50260 (1975Ca40), relative to 100 for 1173 γ . Normalization factor is determined from these values.
I γ normalization: from absolute I(1172.9 γ), weighted average of 0.00337 17 (1971JoZN), 0.00350 21 (1970Va11). Other: 0.0039 4 (1975Ca40). These values are obtained from measured I(1173 γ)/I(γ^+)=0.00172 9 (1971JoZN), 0.00179 11 (1970Va11), theoretical ϵ/β^+ ratios and for different levels populated. Other I(1173 γ)/I(γ^+)=0.00199 (1975Ca40) has not been used - disagrees with values from 1971JoZN and 1970Va11.

E γ †	E(level)	I γ †#	Mult.§	δ §	I($\gamma+ce$)@	Comments
(479.6 $\frac{3}{2}$)	3370.2	0.07 2				I γ : <0.13 (1971JoZN).
(856.2 $\frac{3}{2}$)	3158.1	0.04 2				I γ : <0.11 (1971JoZN).
875.66 7	2048.63	43 2	E2			α =0.000335 5; α (K)=0.000301 5; α (L)=2.96 \times 10 ⁻⁵ 5; α (M)=4.16 \times 10 ⁻⁶ 6; α (N+.)=2.40 \times 10 ⁻⁷ 4. (876 γ)(1173 γ)(θ): A ₂ =+0.38 4, A ₄ =+1.19 8 (1976Ca31).
(968.9 $\frac{3}{2}$)	3270.9	0.09 2				I γ : <0.11 (1971JoZN).
(971 $\frac{3}{2}$)	3861.7	0.03 1				I γ : <0.12 (1971JoZN).
1067.0 10	3370.2	0.19 10				
1128.98 10	2301.95	9.3 5	M1+E2	+3.0 +7-20		δ : from $\gamma\gamma$ (θ) data (1976Ca31), uncertainty at 90% confidence level. (1129 γ)(1173 γ)(θ): A ₂ =-0.31 6, A ₄ =+0.26 12 (1976Ca31). α =0.000181 6; α (K)=0.000161 5; α (L)=1.58 \times 10 ⁻⁵ 5; α (M)=2.22 \times 10 ⁻⁶ 7; α (N+.)=1.00 \times 10 ⁻⁷ 4. α (IPF)=1.88 \times 10 ⁻⁶ 12. α =1.723 \times 10 ⁻⁴ 25; α (K)=1.501 \times 10 ⁻⁴ 21; α (L)=1.466 \times 10 ⁻⁵ 21; α (M)=2.06 \times 10 ⁻⁶ 3; α (N+.)=9.0 \times 10 ⁻⁸ 2. α (IPF)=5.39 \times 10 ⁻⁶ 8.
(1222.3 $\frac{3}{2}$)	3270.9					I γ : <0.08 (1971JoZN).
(1321.6 $\frac{3}{2}$)	3370.2	0.3 1				I γ : <0.11 (1971JoZN).
1717.6 4	2890.6	0.81 12	E2			M=E2(+M1), δ =-4.1 +13-30. α =0.000252 8; α (K)=6.78 \times 10 ⁻⁵ 12; α (L)=6.58 \times 10 ⁻⁶ 12; α (M)=9.27 \times 10 ⁻⁷ 16; α (N+.)=4.5 \times 10 ⁻⁸ 1. α (IPF)=1.77 \times 10 ⁻⁴ 7.
1985.0 10	3158.1	0.30 10	M1+E2	+0.13 8		α =0.000305 5; α (K)=4.94 \times 10 ⁻⁵ 7; α (L)=4.78 \times 10 ⁻⁶ 7; α (M)=6.74 \times 10 ⁻⁷ 10; α (N+.)=3.00 \times 10 ⁻⁸ 5. α (IPF)=2.50 \times 10 ⁻⁴ 4.
(2048.6)	2048.63		E0		0.00109 15	I($\gamma+ce$): from ce(K)(2048 γ)/ce(K)(876 γ)=0.084 11 (1981Pa10) in (p,p' γ).
2084.8 4	3257.7	1.4 3				

Continued on next page (footnotes at end of table)

^{62}Cu ϵ Decay (9.67 min) 1971JoZN,1975Ca40,1970Va11 (continued) $\gamma(^{62}\text{Ni})$ (continued)

$E\gamma^{\dagger}$	E(level)	$I\gamma^{\dagger\#}$	Comments
2097.6 3	3270.9	0.84 11	$\alpha=5.04\times 10^{-4}$ 7; $\alpha(\text{K})=3.97\times 10^{-5}$ 6; $\alpha(\text{L})=3.85\times 10^{-6}$ 6; $\alpha(\text{M})=5.42\times 10^{-7}$ 8; $\alpha(\text{N+..})=2.50\times 10^{-8}$ 4. $\alpha(\text{IPF})=4.59\times 10^{-4}$ 7.
2301.95 8	2301.95	12.3 6	
3158.2 10	3158.1	0.18 4	
3257.3 10	3257.7	0.042 19	
3271.4 4	3270.9	0.21 3	
3370.3 3	3370.2	2.46 14	
3861.7 11	3861.7	0.08 2	

\dagger Weighted averages of values from 1969Es03, 1970Va11, 1971JoZN and 1975Ca40.

\ddagger Expected γ from Adopted Levels, Gammas dataset; not reported in studies of EC decay.

\S From Adopted Gammas, unless otherwise stated.

$\#$ For absolute intensity per 100 decays, multiply by 0.00342 17.

$\textcircled{\#}$ For absolute intensity per 100 decays, multiply by 0.342 17.

^{62}Cu ϵ Decay (9.67 min) 1971JoZN,1975Ca40,1970Val1 (continued)

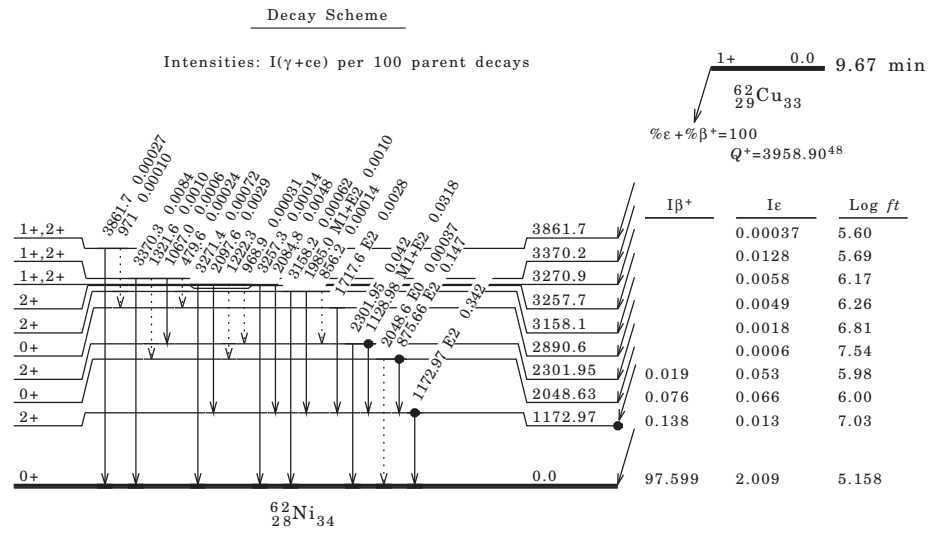


Fig. 10. Nuclear data sheets for the IT decay of $^{99}\text{Tc}^m$ (ENSDF [49]).

$^{99}\text{Tc}_{56}$
 $_{43}\text{Tc}_{56}$

$^{99}\text{Tc}_{56}$
 $_{43}\text{Tc}_{56}$

^{99}Tc IT Decay (6.0067 h)

Parent ^{99}Tc : $E=142.6832$ 11; $J\pi=1/2^-$; $T_{1/2}=6.0067$ h 5; %IT decay=99.9963 6.

The ^{99}Tc isomeric state decays mainly via the 2.17-keV E3 transition which is highly converted. The decay constant depends slightly on the electronic environment of the nucleus. Experimentally studied dependence on chemical state: 1980Ma03, 1972Ni07, 1953Ba41; temperature: 1972Ni07, 1958Be92; pressure (1972Ma27); external electric field: 1970Le25; a theoretical study of these effects together with a review of the experimental results is reported by 1977Do07. See 2004BeZR for evaluated decay data.

For calculation of atomic electron densities and changes in α caused by the chemical and ionization state see 1981Hi03.

The influence of the chemical environment on the conversion electron spectrum has been investigated by 1983Dr15 and 1982Ge01, the influence on $I(K\alpha$ x ray), $I(K\beta$ x ray) by 1981Yo08. $T_{1/2}$ affected by strong radiation (1993Bi15) $T_{1/2}$ for source implanted in Sn and Pb (2000Ko54), chemical influence on $E(\text{ce})$ (1996FiZW)

Others: $T_{1/2}$ 1939Se04, 1950Gl04; $T_{1/2}$ (environment effect): 1960Po04, 1998Ko72. ce 1951Me18, 1951Mi21, 1952Mi38, 1952Sc27, 1956La40, 1958Ch08, 1995Dr08.

^{99}Tc Levels

E(level)	$J\pi$	$T_{1/2}$	Comments
0.0	9/2+		
140.5102 10	7/2+		
142.6836 11	1/2-	6.0067 h 5	$T_{1/2}$: From Adopted Levels.

$\gamma(^{99}\text{Tc})$

$I\gamma$ normalization: From $\Sigma(I(\gamma+\text{ce}))$ to g.s.=99.9963 (6)%, deduced by evaluators assuming an estimated uncertainty of 3% in the relative intensity of $I\gamma(140.5)$. See β^- decay (6.015 h) for β^- branching.

All experiments measuring $E\gamma$ or ce are referenced with ^{99}Mo β^- decay even if a separated ^{99}Tc (6.015 h) source has been used.

Measured Tc K x ray intensity ratios: $K\alpha_2$ x ray/ $K\alpha_1$ x ray=0.528 2, $K\beta_1$ x ray/ $K\alpha_1$ x ray=0.1534 35; $K\beta$ x ray/ $K\alpha$ x ray=0.1776 8 (2007Ya02).

$E\gamma^{\ddagger}$	E(level)	$I\gamma^{\dagger}$	Mult. ‡	δ^{\ddagger}	α	$I(\gamma+\text{ce})^{\dagger}$	Comments
2.1726 4	142.6836		E3		1.37×10^{10}	111.3	ce(M)/($\gamma+\text{ce}$)=0.884 6; ce(N+)/($\gamma+\text{ce}$)=0.1165 22. ce(N)/($\gamma+\text{ce}$)=0.1165 22; ce(O)/($\gamma+\text{ce}$)= 2.54×10^{-6} 5. $I(\gamma+\text{ce})$: deduced from $I(\gamma+\text{ce})(2.17)=I(\gamma+\text{ce})(140.5)$.
140.511 1	140.5102	100 3	M1+E2	+0.129 35	0.113 3		$I\gamma$: Uncertainty in $I\gamma$ has been estimated by evaluators. $\alpha(K)=0.0988$ 25; $\alpha(L)=0.0120$ 5; $\alpha(M)=0.00218$ 8; $\alpha(N+)=0.000367$ 13. $\alpha(N)=0.000345$ 12; $\alpha(O)=2.22 \times 10^{-5}$ 5. $I\gamma$: $I\gamma(140.5)=100$ 3 x 0.89 3=89.0% 3, per 100 decays of ^{99}Tc (6.0 h). The very low uncertainty of 0.3% is due to the covariant relation between the relative γ -ray intensity (100) and the normalization factor (0.89), the latter deduced by evaluators from the decay scheme.
142.63 3	142.6836	0.025 2	M4		40.3		$\alpha(K)=29.2$ 4; $\alpha(L)=9.08$ 13; $\alpha(M)=1.778$ 25; $\alpha(N+)=0.280$ 4. $\alpha(N)=0.269$ 4; $\alpha(O)=0.01071$ 15. $I\gamma$: from ce(K)(142.6)/ce(K)(140.5)=0.075 8 (1969Ag04). Others: 0.021 3 (1980Di16), 0.032 6 (1968Va14), both from ^{99}Mo β^- decay γ -spectra in equilibrium. The prompt components have been subtracted by the evaluators.

† For absolute intensity per 100 decays, multiply by 0.89 3.

‡ See ^{99}Mo β^- decay.

${}^{99}\text{Tc}$ IT Decay (6.0067 h) (continued)

Decay Scheme

Intensities: I(γ +ce) per 100
parent decays
%IT=99.9963 6

